Supporting Information

for

Room-Temperature Phosphorescence-to-Phosphorescence Mechanochromism of a Metal-Free Organic 1,2-Diketone

Yosuke Tani,* Morihisa Terasaki, Mao Komura, Takuji Ogawa*

Department of Chemistry, Graduate School of Science, Osaka University
Machikaneyama 1-1, Toyonaka, Osaka 560-0043, Japan
E-mail: y-tani@chem.sci.osaka-u.ac.jp; ogawa@chem.sci.osaka-u.ac.jp

Table of Contents

1. Instrumentation and Chemicals

Unless otherwise noted, all the reactions were performed in a nitrogen atmosphere using anhydrous solvents and heat-gun-dried glassware on a dual-manifold Schlenk line. ^{1}H and ^{13}C{^{1}H} NMR spectra were recorded on a JEOL ECS400 or ECA500 spectrometer. Chemical shift values (δ) are reported in ppm and are calibrated to tetramethylsilane (0.00 ppm) or residual solvent (7.26 ppm in CDCl$_3$ or 2.05 ppm in (CD$_3$)$_2$CO) for ^{1}H, and to CDCl$_3$ (77.0 ppm) for ^{13}C NMR. Melting points were measured in a glass capillary with a Barnstead/Thermolyne Mel-Temp melting point apparatus. High-resolution mass spectra (ESI-HRMS) were obtained with a Thermo Fisher Scientific LTQ Orbitrap XL mass spectrometer. Elemental analysis was conducted on a Yanaco MT-5 or MT-6 recorder. UV-vis absorption and photoluminescence (PL) spectra in solution were obtained using a Shimadzu UV-3150 spectrometer and a JASCO FP-8200 spectrometer, respectively. Solid-state photoluminescence spectra were obtained using a Hamamatsu photonics C11347-01 spectrometer, a JASCO FP-6500N Spectrofluorometer, or a HORIBA Fluorolog3-211 spectrometer. PL quantum yields were determined in solution by the relative method using quinine sulfate as a standard[1] and in the solid-state samples by the absolute method using a Hamamatsu photonics C11347-01 spectrometer with an integrating sphere. PL lifetime measurements for solid samples were performed using a Hamamatsu photonics C11367-21 fluorescence lifetime spectrometer with a Hamamatsu photonics C11567-02 Xe flash lamp unit for the phosphorescence measurements; for the solution-phase samples, PL lifetimes were obtained using a HORIBA Fluorolog3-211 spectrometer. Low-temperature PL spectra were obtained using a JASCO FP-6500N spectrometer with a L42 sharp cut filter (long pass, >420 nm). Analytical thin-layer chromatography (TLC) was performed on aluminum plates bearing a layer of Merck silica gel 60 F$_{254}$. Column chromatography was carried out on silica-gel (Kishida Chemical Co., Ltd, spherical, neutral, 63–200 μm).

Anhydrous THF and CH$_2$Cl$_2$ were purchased from Wako Chemical Co., Inc. and Kanto Chemical Co., Inc., respectively, and further purified by passage through activated alumina under positive nitrogen pressure as described by Grubbs et al.[2] Unless otherwise noted, chemicals obtained from commercial suppliers were used without further purification.
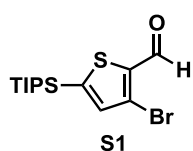
2. Synthesis Procedures for Thenils 1–3
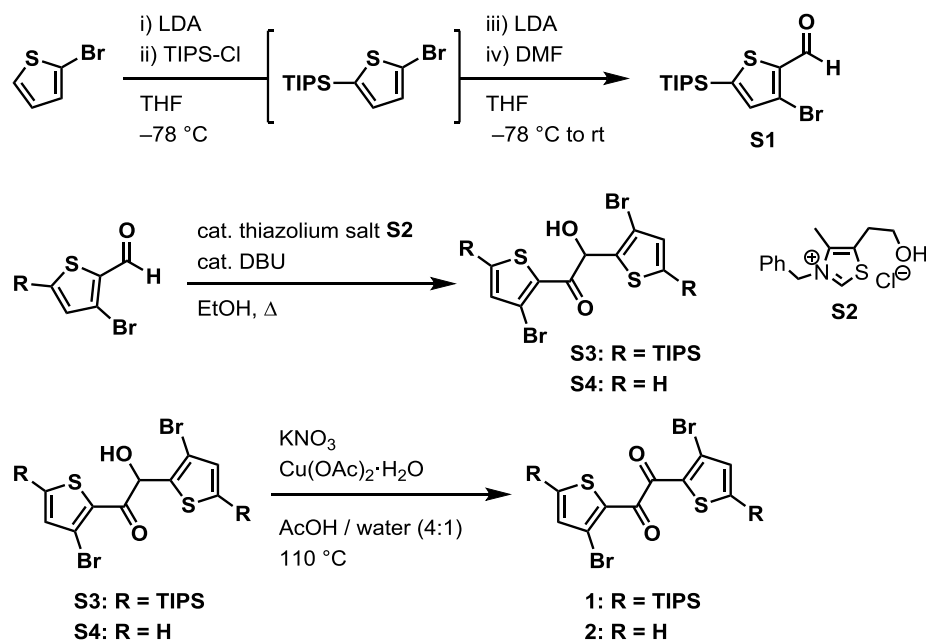
LDA = lithium diisopropylamide; TIPS = triisopropylsilyl; DMF = *N*,*N*-dimethylformamide;
DBU = 1,8-diazabicyclo[5.4.0]undec-7-ene

Scheme S1. Synthesis of Thenils 1 and 2

3-bromo-2-formyl-5-(triisopropylsilyl)thiophene (S1)

To a 50 mL 2-neck flask were added diisopropylamine (2.8 mL, 19.8 mmol) and THF (10 mL). The flask was cooled to –30 °C and butyllithium (BuLi, 2.65 M in hexane, 7.4 mL, 19.6 mmol) was added dropwise. The mixture was stirred for 20 min at 0 °C to prepare the lithium diisopropylamide (LDA) solution. To another 200 mL 2-neck flask were added 2-bromothiophene (3.26 g, 20 mmol) and THF (50 mL). The flask was cooled to –78 °C and freshly prepared LDA solution (cooled to –78 °C) was added dropwise via cannula. The mixture was stirred for 30 min at the same temperature before triisopropylsilylchloride (4.2 mL, 20 mmol) was added dropwise; stirring was continued for 1 h at the same temperature to form 2-bromo-5-(triisopropylsilyl)thiophene. LDA was again prepared by the same method from diisopropylamine (3.0 mL, 21 mmol), BuLi (2.65 M in hexane, 7.8 mL, 21 mmol), and THF (10 mL). To the reaction mixture containing thiophene was transferred LDA dropwise via cannula at –78 °C. The resulting mixture was stirred for 1 h, and then DMF (1.9 mL, 24.7 mmol) was added dropwise. After 15 min, the mixture was warmed to room temperature and stirred overnight. The reaction was quenched by

adding aq. NH_4Cl (50 mL) and Et_2O (100 mL). The organic layer was separated and the aqueous layer was extracted with Et_2O (50 mL × 3). The combined organic extracts were washed with brine, dried over $MgSO_4$, filtered and then evaporated. The residue was purified by silica-gel column chromatography (eluent: hexane to hexane/EtOAc 10%) to give **S1** (6.02 g, 88%) as a yellow-orange solid, which included less than 4% of 2-bromo-5-formylthiophene. This can be further purified by recrystallization from hexane in a refrigerator to give pure **S1** as a white solid. **¹H NMR** (400 MHz, $CDCl_3$) δ: 9.96 (s, 1H), 7.23 (s, 1H), 1.42–1.31 (m, 3H), 1.11 (d, $J = 7.3$ Hz, 18H). **¹³C NMR** (100 MHz, $CDCl_3$) δ: 182.5, 147.2, 140.7, 139.0, 138.9, 120.6, 18.3, 11.5. **ESI-HRMS** (*m/z*): [M+H]⁺ calcd for $C_{14}H_{24}BrOSSi$, 347.0495; found, 347.0497. All the resonances in the ¹H and ¹³C NMR spectra were in good agreement with reported data.[3]

1,2-bis[3-bromo-5-(triisopropylsilyl)thiophen-2-yl]-2-hydroxyethan-1-one (S3)
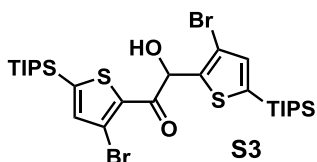
To a Schlenk tube were added **S1** (2.08 g, 6.0 mmol), thiazolium salt **S2** (81 mg, 0.30 mmol), and EtOH (2 mL). The tube was shortly evacuated and backfilled with N_2 three times, after which 1,8-diazabicyclo[5.4.0]undec-7-ene (DBU, 60 µL, 0.40 mmol) was added. The mixture was stirred for 16 h at 70 °C, and then quenched by adding aq. NH_4Cl and Et_2O at room temperature. The organic layer was separated and the aqueous layer was extracted with Et_2O. The combined organic extracts were dried over $MgSO_4$, filtered and then evaporated. The residue was purified by silica-gel column chromatography (eluent: hexane/CH_2Cl_2 2:1 to 1:1) to give **S3** (1.30 g, 63%) as a yellowish oil, which was solidified upon standing. **¹H NMR** (500 MHz, $CDCl_3$) δ: 7.16 (s, 1H), 7.08 (s, 1H), 6.03 (d, $J = 5.3$ Hz, 1H), 4.53 (d, $J = 5.3$ Hz, 1H), 1.33–1.21 (m, 6H), 1.06–1.00 (m, 36H). **¹³C NMR** (125 MHz, $CDCl_3$) δ: 188.8, 145.7, 140.2, 139.8, 138.0, 137.8, 135.4, 118.6, 114.6, 71.8, 18.3, 18.3, 11.4. **ESI-HRMS** (*m/z*): [M+Na]⁺ calcd for $C_{28}H_{46}O_2Br_2S_2Si_2Na$, 715.0740; found, 715.0742. All the resonances in the ¹H and ¹³C NMR spectra were in good agreement with reported data.[3]

1,2-bis(3-bromothiophen-2-yl)-2-hydroxyethan-1-one (S4)
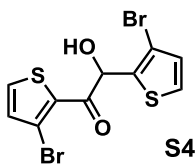
Synthesized in 55% yield from 3-bromothiophene-2-carboxyaldehyde (511 mg, 2.67 mmol) using thiazolium salt **S2** (41 mg, 0.15 mmol) and DBU (30 µL, 0.30 mmol) at 70 °C for 4 h. **¹H NMR** (400 MHz, $CDCl_3$) δ: 7.56 (d, $J = 5.3$ Hz, 1H), 7.32 (dd, $J = 5.3, 0.7$ Hz, 1H), 7.12 (d, $J = 5.3$ Hz, 1H), 7.00 (d, $J = 5.3$ Hz, 1H), 6.13 (dd, $J = 6.2, 0.7$ Hz, 1H), 4.38 (app d, $J = 6.2$ Hz, 1H). **¹³C NMR** (100 MHz, $CDCl_3$) δ: 189.1, 135.2, 133.8, 133.7, 131.7, 130.7,

127.6, 118.5, 113.6, 71.4. **ESI-HRMS** (*m/z*): [M+Na]$^+$ calcd for $C_{10}H_6O_2Br_2\,S_2Na$, 402.8068; found, 402.8066. All the resonances in the ^1H and ^{13}C NMR spectra were in good agreement with reported data.[3]

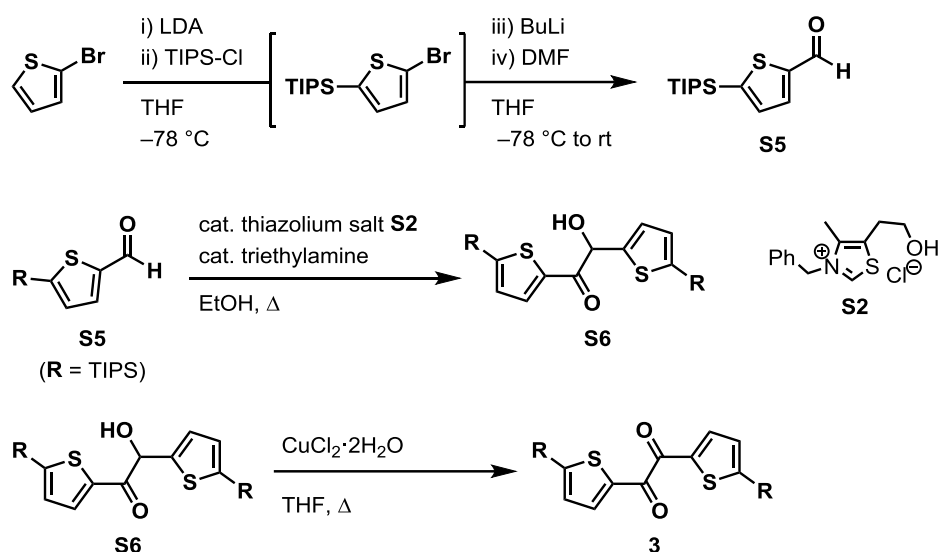### 1,2-bis(3-bromo-5-(triisopropylsilyl)thiophen-2-yl)ethane-1,2-dione (1)
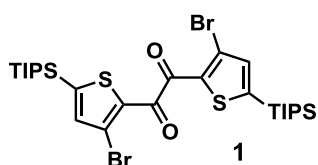
To a 50 mL flask were added **S3** (845 mg, 1.22 mmol), KNO_3 (155 mg, 1.53 mmol), $Cu(OAc)_2 \cdot H_2O$ (4.2 mg, 21 μmol), and $AcOH/H_2O$ (4:1, 4.0 mL). The mixture was stirred overnight at 110 °C. After cooling to room temperature, the mixture was quenched by adding H_2O and CH_2Cl_2. The organic layer was separated and the aqueous layer was extracted with CH_2Cl_2 three times. The combined organic extracts were dried over $MgSO_4$, filtered and then evaporated. The residue was purified by recrystallization from a stirred solution in $CHCl_3$ by adding methanol at room temperature to give pure **1** (823 mg, 97%) as a slightly yellow powder. **m.p.**157–160 °C. ^{1}**H NMR** (500 MHz, $(CD_3)_2CO$) δ: 7.50 (s, 2H), 1.52–1.43 (m, 6H), 1.17 (d, *J* = 7.4 Hz, 36H). ^{13}**C NMR** (125 MHz, $CDCl_3$) δ: 182.2, 149.3, 140.3, 136.1, 119.8, 18.4, 11.6. **Anal.** Calcd for $C_{28}H_{44}Br_2O_2S_2Si_2$: C, 48.55; H, 6.40. Found: C, 48.44; H, 6.27. Single crystal of **1** (CCDC-1906440) was obtained by vapor diffusion of $CHCl_3$/hexane.

### 1,2-bis(3-bromothiophen-2-yl)ethane-1,2-dione (2)
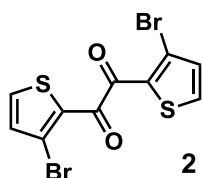
To a 50 mL flask were added **S4** (500 mg, 1.3 mmol), KNO_3 (97 mg, 0.96 mmol), $Cu(OAc)_2 \cdot H_2O$ (1.7 mg, 8 μmol) and $AcOH/H_2O$ (4:1, 1.0 mL). The mixture was stirred for 2.5 h at 110 °C. After cooling to room temperature, the mixture was quenched by adding H_2O and $CHCl_3$. The organic layer was separated and the aqueous layer was extracted with $CHCl_3$ three times. The combined organic extracts were dried over $MgSO_4$, filtered and then evaporated to give **2** as an orange solid (472 mg, 92%). **m.p.**175–177 °C. ^{1}**H NMR** (400 MHz, $CDCl_3$) δ: 7.77 (d, *J* = 5.0 Hz, 2H), 7.20 (d, *J* = 5.3 Hz, 2H). ^{13}**C NMR** (125 MHz, $CDCl_3$) δ: 182.6, 136.5, 133.3, 132.2, 119.7. **Anal.** Calcd for $C_{10}H_4Br_2O_2S_2$: C, 31.60; H, 1.06. Found: C, 31.89; H, 1.21. Single crystal of **2** (CCDC-1906439) was obtained by vapor diffusion of $CHCl_3$/hexane.

2,2'-Dibromobenzil was synthesized from 2,2'-dibromobenzoin[4] (740 mg, 2.0 mmol) in 79% yield (580 mg) in a similar manner to **1** and **2**. All the resonances in the ^1H and ^{13}C NMR spectra were in good agreement with reported data.[5]

Scheme S2. Synthesis of Thenil 3

## 2-formyl-5-(triisopropylsilyl)thiophene (S5)
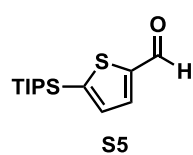
To a 50 mL 2-neck flask were added diisopropylamine (3.6 mL, 26 mmol) and THF (12 mL). The flask was cooled to –30 °C and BuLi (2.65 M in hexane, 9.4 mL, 25 mmol) was added dropwise. The mixture was stirred for 10 min at 0 °C to prepare LDA solution. To another 200 mL 2-neck flask were added 2-bromothiophene (4.0 g, 25 mmol) and THF (62 mL). The flask was cooled to –78 °C and freshly prepared LDA solution (cooled to –78 °C) was added dropwise via cannula. The mixture was stirred for 30 min at the same temperature before triisopropylsilylchloride (5.3 mL, 25 mmol) was added dropwise; stirring was continued for 1 h at the same temperature to form 2-bromo-5-(triisopropylsilyl)thiophene. To the reaction mixture containing thiophene was added dropwise BuLi (2.65 M in hexane, 10 mL, 27 mmol) at –78 °C. The resulting mixture was stirred for 1 h, and then DMF (2.2 mL, 29 mmol) was added dropwise. After 20 min, the mixture was warmed to room temperature and stirred overnight. The reaction was quenched by adding aq. NH$_4$Cl and Et$_2$O. The organic layer was separated and the aqueous layer was extracted with Et$_2$O three times. The combined organic extracts were washed with brine, dried over MgSO$_4$, filtered and then evaporated. The residue was purified by silica-gel column chromatography (hexane/EtOAc, 12:1) to give **S5** (2.11 g, 32%) as a yellow-orange solid. **^{1}H NMR** (400MHz, CDCl$_3$) δ: 9.96 (s, 1H), 7.83 (d, J = 3.7 Hz, 1H), 7.34 (d, J = 3.7 Hz, 1H), 1.41-1.35 (m, 3H), 1.11 (d, J = 7.3 Hz, 18H).**^{13}C NMR** (100 MHz CDCl$_3$) δ: 182.4, 148.3, 147.2, 136.4, 136.1, 18.4, 11.6.

1,2-bis[5-(triisopropylsilyl)thiophen-2-yl]-2-hydroxyethan-1-one (S6)
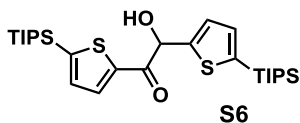
To a Schlenk tube were added **S5** (0.81 g, 3.0 mmol), thiazolium salt **S2** (45 mg, 0.15 mmol), and EtOH (1.0 mL). The tube was shortly evacuated and backfilled with N_2 five times, after which triethylamine (30 μL, 0.21 mmol) was added. The mixture was stirred at 70 °C overnight, and then quenched at room temperature by adding NH_4Cl aq. and Et_2O. The organic layer was separated and the aqueous layer was extracted with Et_2O three times. The combined organic extracts were dried over $MgSO_4$, filtered, and then evaporated. The residue was purified by silica-gel column chromatography (hexane/EtOAc, 14:1) to give **S6** (0.23 g, 28%) as a slightly yellow oil. **^{1}H NMR** (400 MHz CDCl$_3$) δ: 7.80 (d, J = 3.9 Hz, 1H), 7.23 (d, J = 3.9 Hz, 1H), 7.16 (dd, J = 3.4, 0.5 Hz, 1H), 7.12 (d, J = 3.4 Hz, 1H), 6.03 (d, J = 5.5 Hz, 1H), 4.46 (d, J = 6.0 Hz, 1H), 1.40-1.22 (m, 6H), 1.08-1.05 (m, 40H). **^{13}C NMR** (100MHz CDCl3) δ: 189.55, 147.24, 146.80, 143.43, 136.09, 135.94, 135.66, 134.42, 127.78, 71.77, 18.44, 18.34, 11.62, 11.56.

1,2-bis(5-(triisopropylsilyl)thiophen-2-yl)ethane-1,2-dione (3)
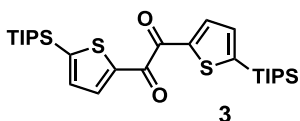
To a 50 mL flask were added **S6** (0.30 g, 0.57 mmol), THF (2.0 mL), and $CuCl_2·H_2O$ (0.19 g, 1.1 mmol). The mixture was stirred for 1 h at 80 °C. After cooling to room temperature, the mixture was quenched by adding H_2O and washed with aq. $Na_2S_2O_3$. The organic layer was separated and the aqueous layer was extracted with Et_2O three times. The combined organic extracts were washed with aq. NH_4Cl, and the aqueous layer was extracted with Et_2O three times. The combined organic extracts were dried over $MgSO_4$, filtered, and then evaporated. The residue was purified by recrystallization from a stirred solution in CHCl$_3$ by adding methanol at room temperature to give pure **3** (0.19 g, 63%) as a slightly yellow powder. **m.p.**113–114 °C. **^{1}H NMR** (400 MHz CDCl$_3$) δ: 8.08 (d, J = 3.9 Hz, 1H), 7.33 (d, J = 3.9 Hz, 1H), 1.43-1.35 (m,2H), 1.12 (d, J = 7.5 Hz, 15H) **^{13}C NMR** (100MHz CDCl3) δ: 182.6, 150.1, 143.2 137.2, 136.5, 18.5, 11.7. **Anal.** Calcd for $C_{28}H_{46}O_2S_2Si_2$: C, 62.49; H, 9.01. Single crystal of **3** (CCDC-1906441) was obtained by slow-cooling of hot hexane solution.

3. Stimuli-Responsive Behavior of Thenils 1–3

Heat- and vapor-induced transition from 1Y to 1G

1G was prepared by recrystallization from a stirred solution of **1** (104 mg) in $CHCl_3$ (3 mL) by drop-wise addition of methanol (12 mL) at room temperature. **1Y** was obtained by uniformly grinding **1G** for 30 min with an agate mortar and pestle.

To evaluate the heat-induced recovery of **1Y**, three samples were prepared; **1Y-h1**, at 100 °C for 1 h; **1Y-h2**, at 120 °C for 19 h; **1Y-h3**, at 120 °C for 22 h. Each samples was placed on a cover glass and heated on a hot plate. After heating, the samples were cooled to room temperature on the hot plate with the switch turned off. For the evaluation of the solvent vapor-induced recovery, two vials, containing **1Y** and $CHCl_3$, respectively, were inserted in an upside-down TLC expansion tank and maintained inside it for 1h (**1Y-f1**), 19 h (**1Y-f2**) or 22 h (**1Y-f3**).

Photoluminescence (PL) spectra were measured with a Hamamatsu photonics C11347-01 spectrometer for **1G** and **1Y**, and a HORIBA Fluorolog3-211 spectrometer for **1Y-h** and **1Y-f**. These samples were excited at 360 nm. Powder X-ray diffraction (PXRD) patterns were collected on a Rigaku SmartLab Multi-purpose X-ray diffractometer with CuKα radiation (λ = 1.5418 Å) using D/teX as a detector. Photographs were taken using SONY NEX-5N.

As a result of heating or fumigation, emission color appeared, by naked eyes, to turn back to yellow-green from yellow (Figure S1). The PL spectra showed increases in intensity at 520 nm with fumigation or heating time, although the PL spectra of **1Y-h3** and **1Y-f3** did not completely match that of **1G** (Figures S2 and S3). The PXRD data of **1Y-h3** and **1Y-f3** revealed distinct sharp patterns matching those of **1G** (Figure S4). These results indicate that **1Y** reverted to **1G** when it was exposed to $CHCl_3$ vapor or heated.

It should be remarked that the diffraction peak at $2\theta = 6.2°$ corresponds to the (002) plane, which sits between the triisopropylsilyl (TIPS) groups of neighboring molecules (Figure 2e right in the main text). Considerable decrease of this peak upon grinding, and moderate recovery upon fumigation or heating, imply that the atoms around this plane readily loose thier periodicity and are disordered after recovery.
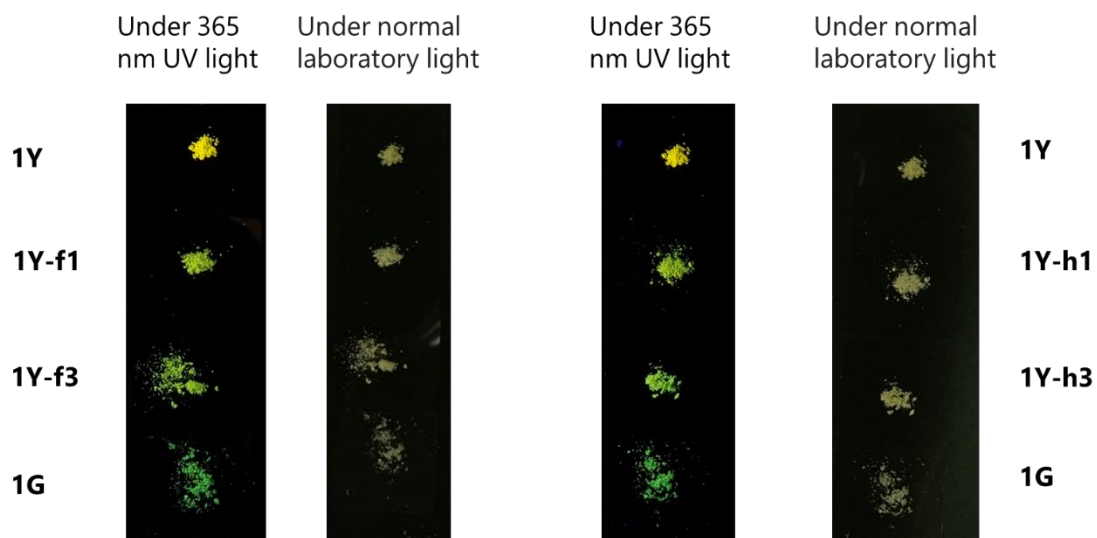
Figure S1. Heat-induced and solvent vapor-induced recovery of **1Y**. These photographs were taken under irradiation with UV light (365 nm) and with normal laboratory light.
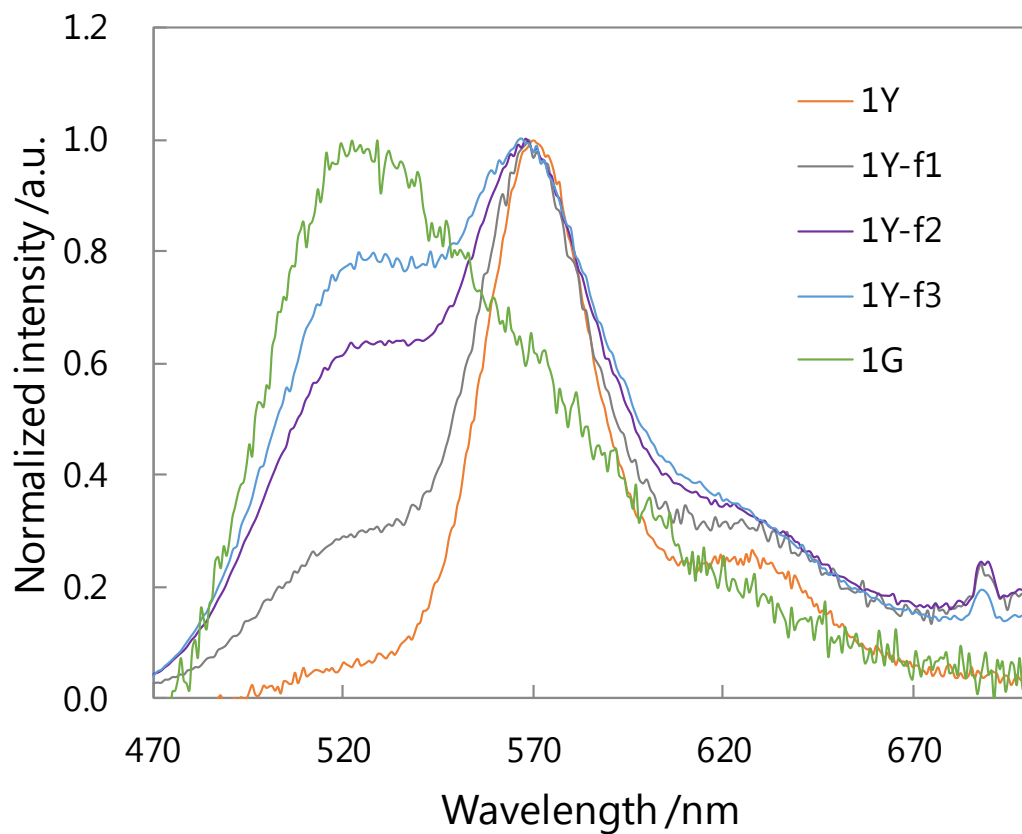

Figure S2. Normalized PL spectra of **1Y** (orange), **1Y-f1** (gray), **1Y-f2** (purple), **1Y-f3** (blue), and **1G** (green).
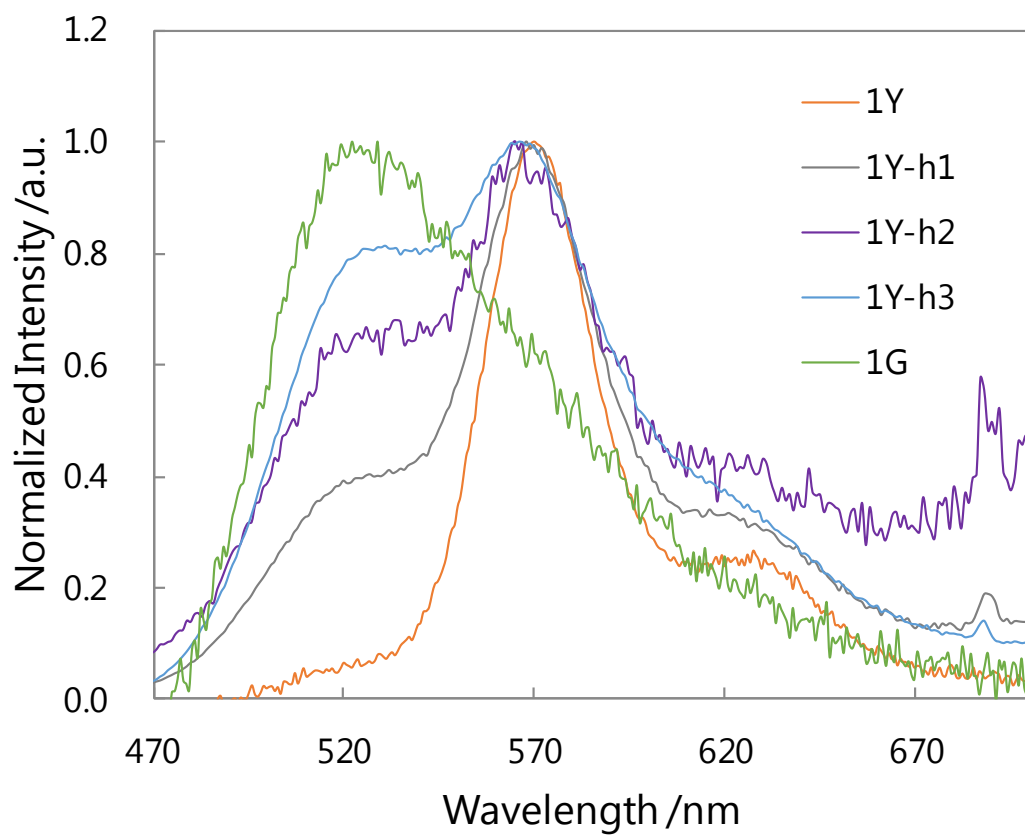
Figure S3. Normalized PL spectra of **1Y** (orange), **1Y-h1** (gray), **1Y-h2** (purple), **1Y-h3** (blue), and **1G** (green).
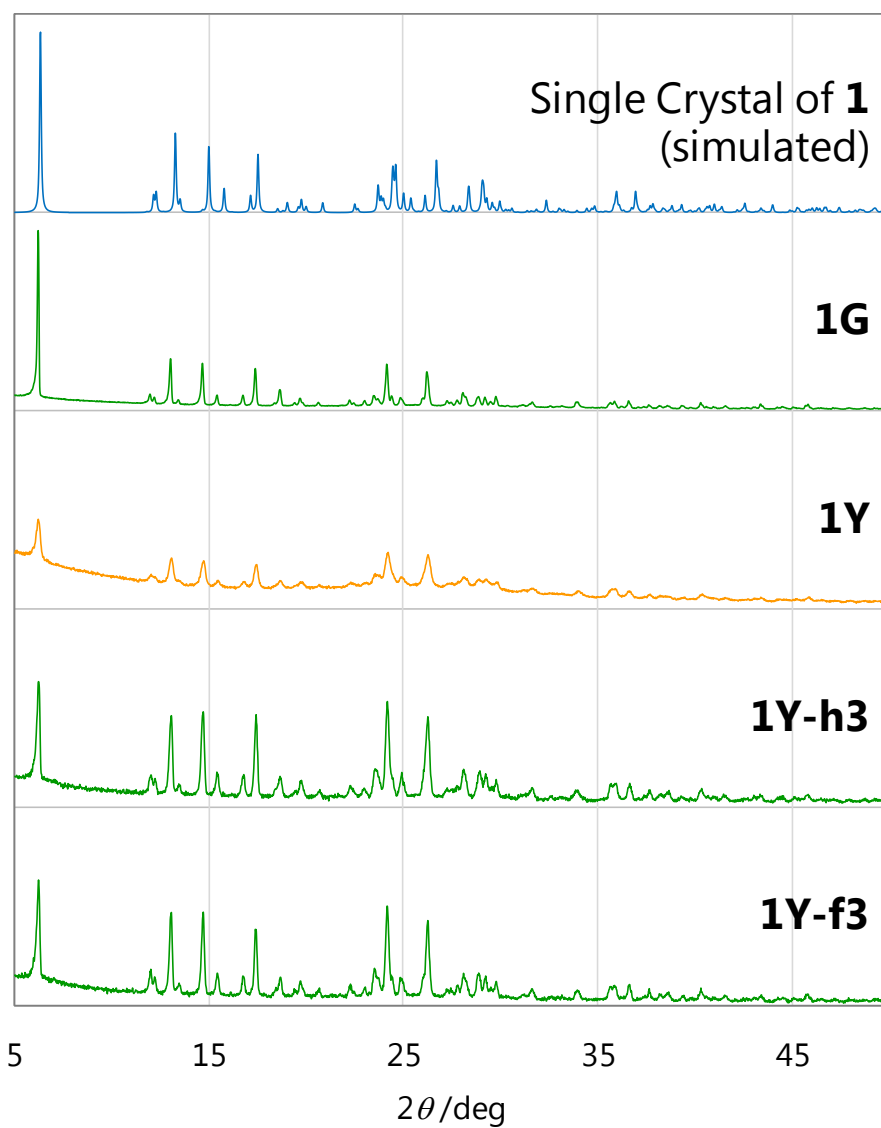
Figure S4. PXRD profiles of (from top to bottom) single crystal of **1** (simulated), **1G**, **1Y**, **1Y-h3**, and **1Y-f3**.

Mechano-responsive behavior of 2 and 3

Thenil **2**, which has H in place of TIPS groups in **1**, is not emissive both in crystal and after grinding. On the other hand, thenil **3**, which has H in place of Br atoms in **1**, shows green emission but no mechano-responsive behavior.
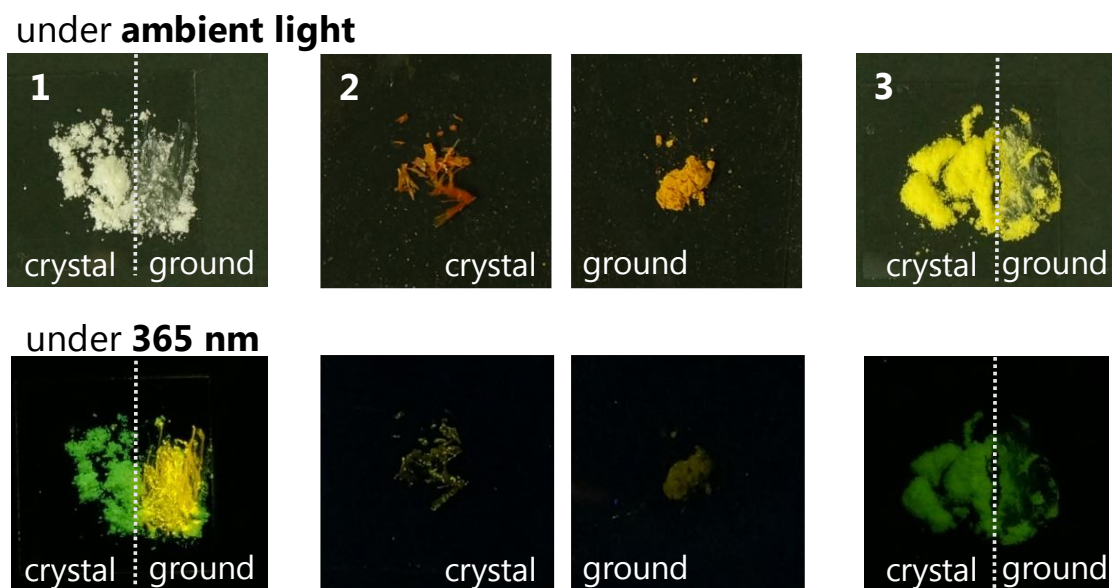

Figure S5. Mechano-responsive behavior of **1**, **2**, and **3**. Photographs were taken under normal laboratory light (top) and under irradiation with UV light (365 nm).

4. Single Crystal X-ray Structure Analysis

Data were collected on a Rigaku VariMax RAPID FR-E diffractometer using multilayer mirror monochromated Mo Kα radiation ($\lambda = 0.71075$ Å) in the ω-scan mode. The crystals were cooled by a stream of cold N_2 gas. Collection, indexing, peak integration, cell refinement, and scaling of the diffraction data were performed using the RAPID AUTO software (Rigaku). The structures were solved by direct methods (SIR97) and refined by full-matrix least-square refinement on F^2 (SHELXL2014). The non-hydrogen atoms were refined anisotropically. All hydrogen atoms were placed on the calculated positions and refined using the riding model.

Table S1. Crystallographic Data for 1–3

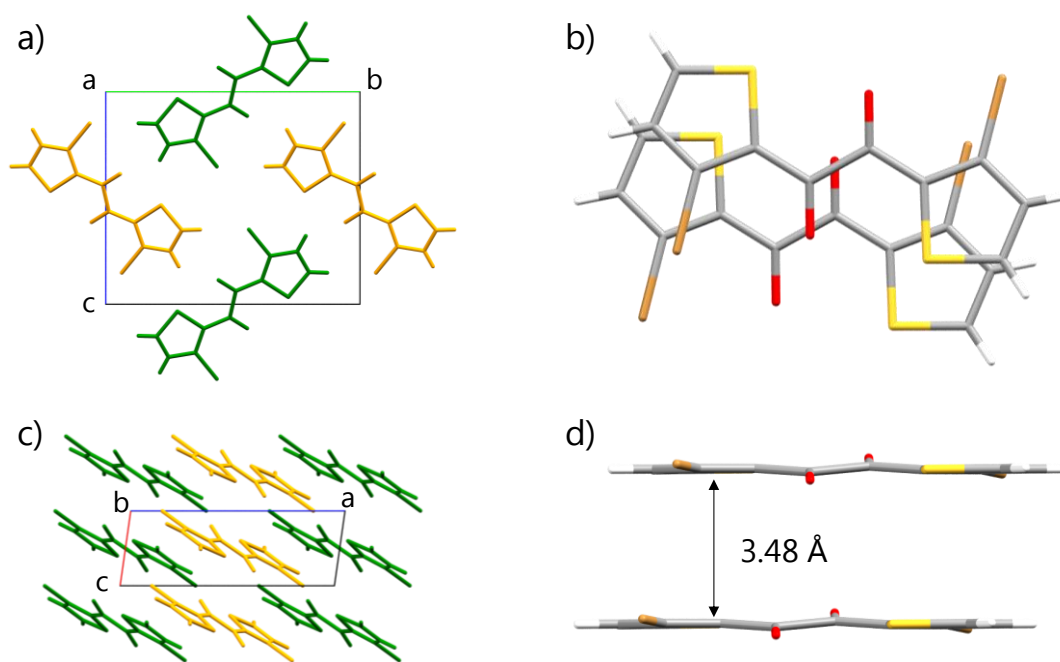|	1	2	3
Empirical formula	$C_{28}H_{44}Br_2O_2S_2Si_2$	$C_{10}H_4Br_2O_2S_2$	$C_{28}H_{46}O_2S_2Si_2$
FW	692.75	380.07	534.95
T (K)	123(2)	123(2)	123(2)
Crystal system	Monoclinic	Monoclinic	Monoclinic
Space group	$C\,2/c$	$P\,2_1/c$	$P\,2_1/c$
a (Å)	12.0795(9)	3.8748(3)	14.8648(5)
b (Å)	9.5698(6)	13.0602(10)	14.9373(4)
c (Å)	27.9836(17)	11.0151(10)	15.6032(4)
α (deg)	90	90	90
β (deg)	92.019(7)	98.117(7)	117.170(8)
γ (deg)	90	90	90
V (Å^3)	3232.9(4)	551.84(8)	3082.2(2)
Z	4	2	4
D (calcd) g·cm^{-3}	1.423	2.287	1.153
Crystal size (mm^3)	$0.09 \times 0.09 \times 0.03$	$0.14 \times 0.11 \times 0.07$	$0.17 \times 0.14 \times 0.07$
Completeness	99.9 %	99.9%	99.9%
GOF on F^2	1.017	1.001	1.098
$R_1\ [I > 2\sigma(I)]$	0.0304	0.0248	0.0295
wR_2 (all data)	0.0641	0.0534	0.0874

Figure S6. Packing structure of **2** seen along the a-axis (a) and b-axis (c), and perpendicular to (b) and along (d) the molecular mean plane.
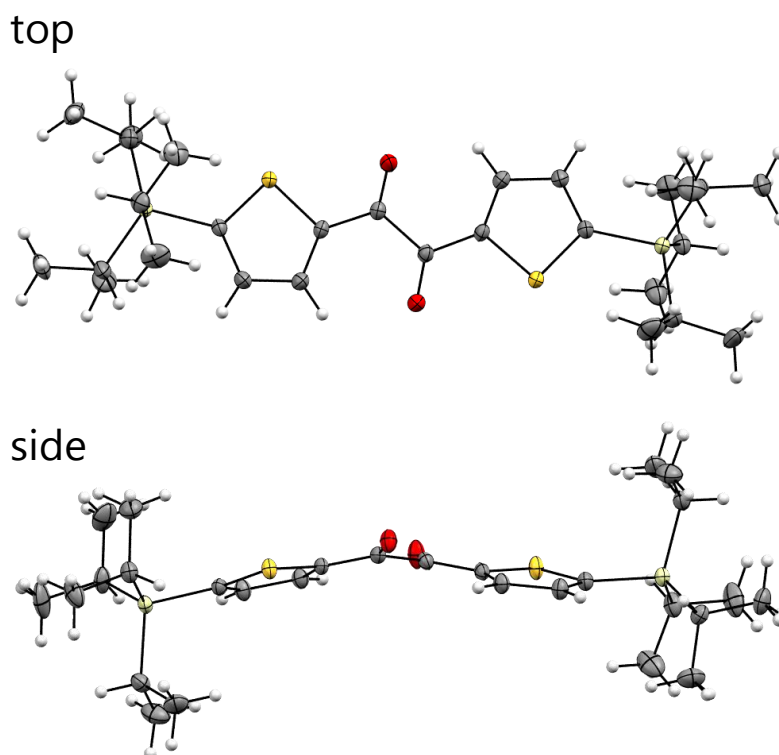

Figure S7. Crystal structure of **3**. The dihedral angle of the vicinal dicarbonyl is 153°.

5.　Photophysical Properties

UV-vis absorption and photoluminescence (PL) spectra in solution

　　For the measurement of UV-vis absorption, an analytically pure sample was dissolved in spectral-grade solvents so that the concentrations were of the order of 10^{-5} M. The solution was further diluted to 10 times for PL measurement. The samples were degassed by bubbling N_2 through them for 30 min. Note that even with highly diluted 4×10^{-7} M solution of **1** the PL spectrum did not changed and no RTP from the skew conformer was observed. In addition, excitation spectrum matched well with corresponding absorption spectrum. These results indicate that energy transfer is unlikely in solution.
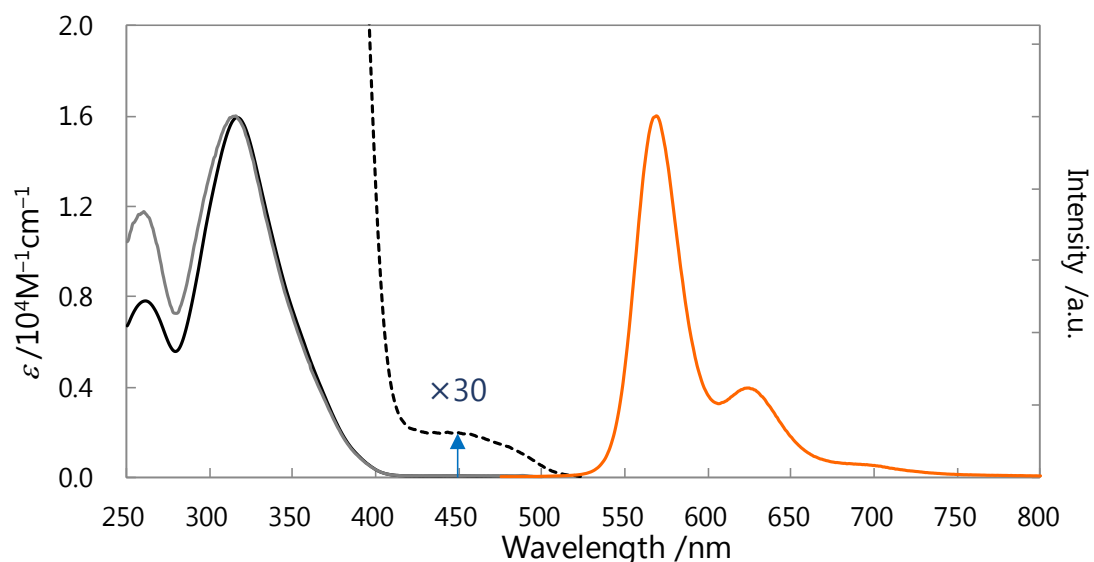
Figure S8. UV-vis absorption (black), excitation (grey, λ_{ex} = 570 nm), and PL spectra (orange, λ_{ex} = 320 nm) of **1** in cyclohexane. The left axis indicates molar absorption coefficient and the right axis indicates normalized excitation and emission intensity. The UV-vis absorption spectrum of the concentrated solution (of the order of 10^{-4} M) enlarged by thirty times is also shown as the broken line.
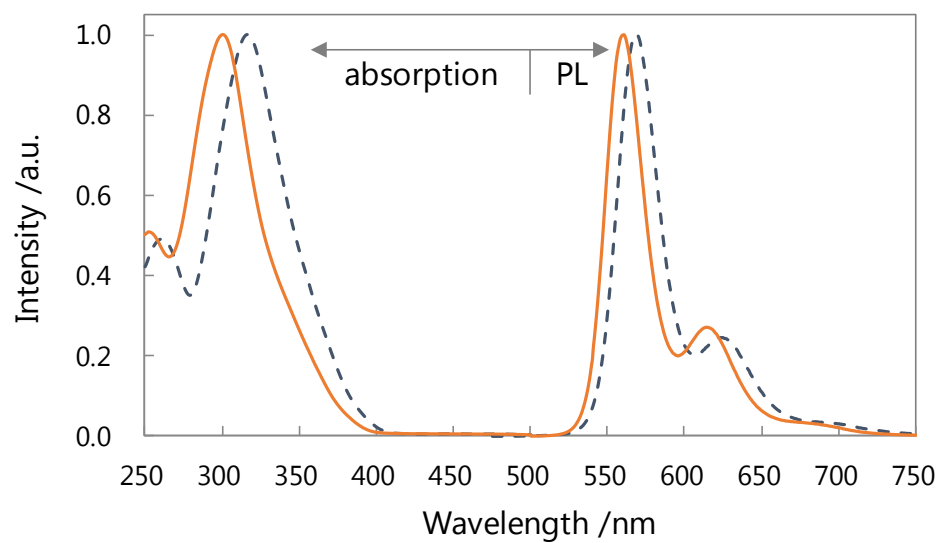
Figure S9. UV-vis absorption and normalized PL spectra (λ_{ex} = 320 nm) of **2** (orange lines) and **1** (black broken lines) in cyclohexane.
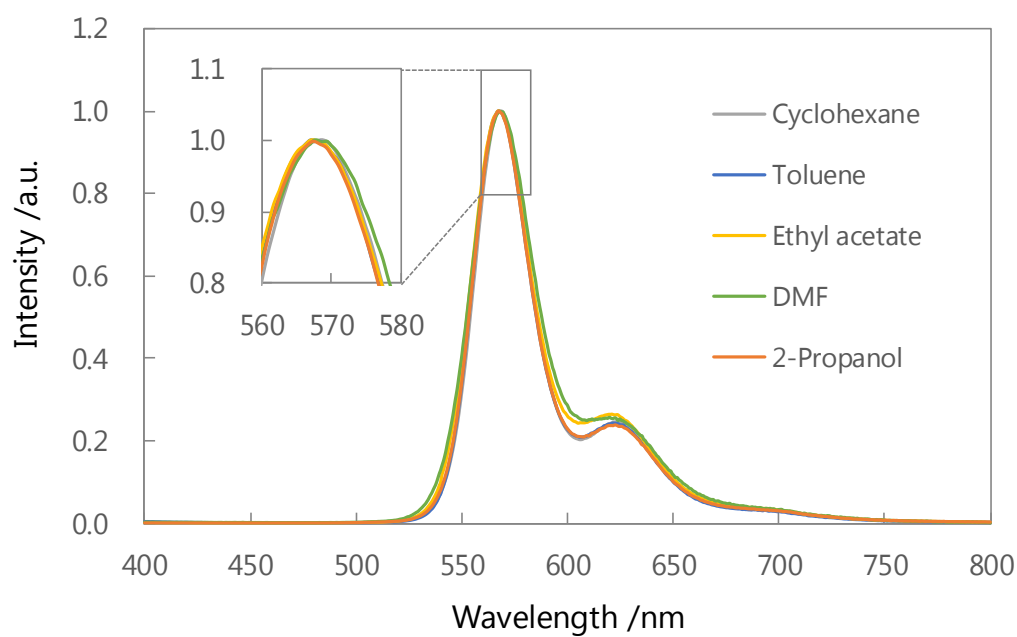

Figure S10. Normalized PL spectra of **1** in various solvents (λ_{ex} = 320 nm).

Table S2. UV-vis Absorption and PL Properties of 1 in Various Solvents and Corresponding Data for 1G and 1Y

sample	λ_{abs} (nm)^a	λ_{em} (nm)^b	Φ in N$_2$^{c}	Φ in air
In cyclohexane	316	569	0.13	0.02^c
In toluene	318	567	0.10	0.02^c
In ethyl acetate	315	568	0.05	0.01^c
In DMF	318	568	0.02	<0.01^c
In 2-propanol	325	568	—^{d}	—^{d}
1G		522		0.04^{e,f}
1Y		569		0.10^{e,g} (0.06^{e,h})

^{a}Wavelength of the global absorption maximum. ^{b}Wavelength of the global emission maximum. ^{c}Determined relative to quinine sulfate (0.60 in 0.05 M H$_2$SO$_4$). Excited at 320 nm. ^{d}Not determined because of its poor solubility. ^{e}Determined using an integrating sphere. ^{f}Independent to the excitation wavelength from 300 to 400 nm. ^{g}Excited at 370 nm. ^{h}Excited at 320 nm.

Low-temperature PL spectra

We measured PL spectra of **1Y** and single crystal of **1** at 77 K (λ_{ex} = 360 nm) using a JASCO FP-6500N spectrometer with a L42 sharp cut filter (long pass, >420 nm).

The spectrum of **1Y** at 77 K exhibited a dual emission with λ_{em} = 524 and 570 nm (Figure S11b). Time-gated phosphorescence measurements revealed that the new peak with λ_{em} = 524 nm decays slower than the TP emission does (Figure S11c), and the spectrum with 10 ms delay (Figure S11d) was identical to a steady-state PL spectrum of **1** single crystal at 77 K (Figure S11e). These results indicate that both the skew and TP conformers are present in **1Y**, and that the emission from the skew conformer is quenched at room temperature.
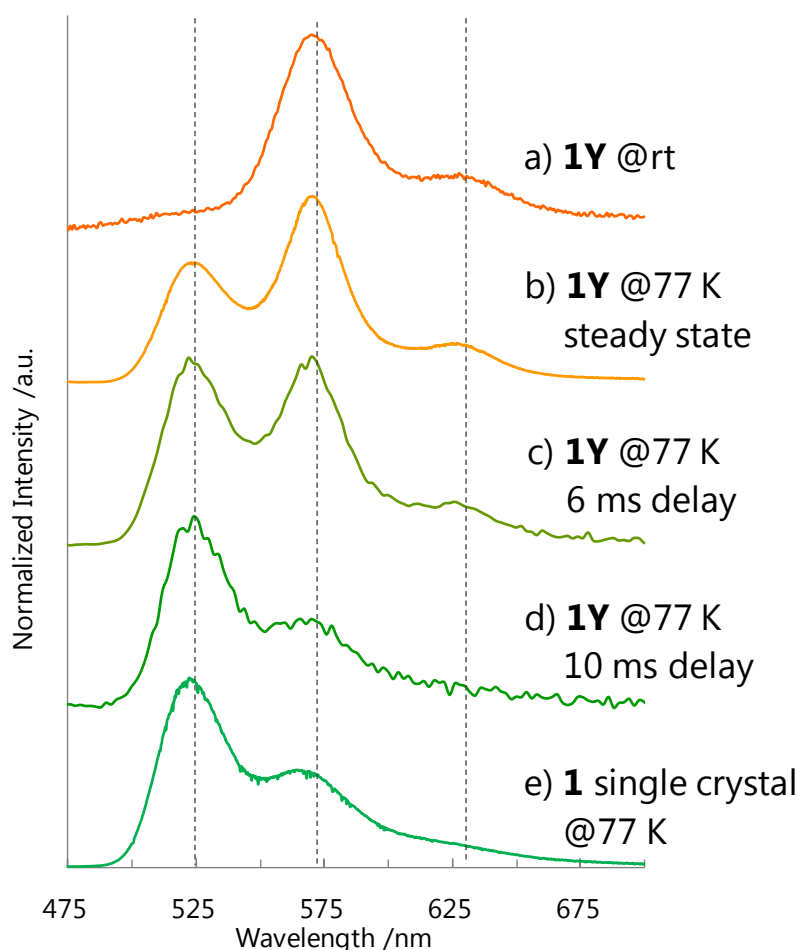

Figure S11. Steady state and delayed PL spectra of **1Y** at room temperature or 77 K, and steady state PL spectrum of single crystal **1** at 77 K (λ_{ex} = 360 nm).

Absorption and excitation spectra of 1G and 1Y

We measured diffuse reflectance spectra using a SHIMADZU UV-3150 spectrometer and a SHIMADZU ISR-3100 integrating sphere attachment. Single crystal of **1** (**1SC**) was embedded in a BaSO$_4$ plate and **1Y** was mixed with BaSO$_4$. Kubelka-Munk conversion of these spectra gave solid-state absorption spectra. Excitation spectra of **1G** and **1Y** were measured using a JASCO FP-8200 spectrometer.

The absorption spectrum of **1SC** had a broader red-shifted peak compared to that of **1** in cyclohexane (Figure S12 top). The observed red shift is probably due to intermolecular electronic interactions in the well-ordered crystalline state. The excitation spectrum of **1G** monitored at $\lambda_{em} = 520$ nm was quite similar to the absorption spectra of **1SC**. These results indicate that, in **1G**, the skew conformer is excited and then emits green RTP. The absorption spectrum of **1Y** was blue-shifted compared to that of **1G** (Figure S12 bottom), possibly due to the disappearance of intermolecular electronic interactions in **1Y**. The excitation spectrum of **1Y** has a non-negligible intensity in the region 300–340 nm, implying that the skew conformer also contributes to the emission.
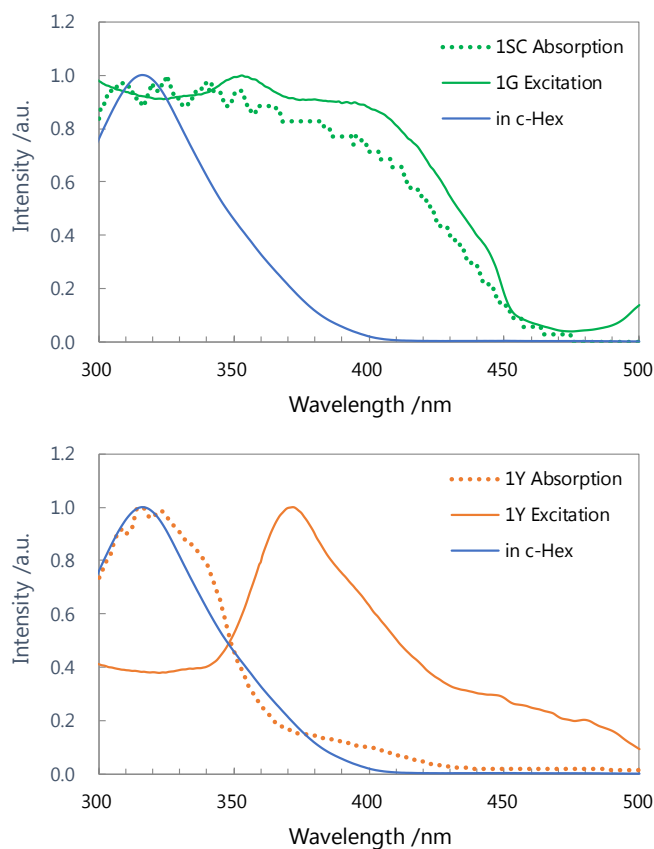

Figure S12. Absorption spectra of **1** in cyclohexane (blue), **1SC** (green dotted line), and **1Y** (orange dotted line). Excitation spectra of **1G** (green) and **1Y** (orange).

PL lifetime of 1 in solution

Analytically pure **1** was dissolved in cyclohexane so that the concentration was in the order of 10^{-6} M, and degassed by N_2 bubbling for 35 min. The photoluminescence decay curve was measured with a HORIBA Fluorolog3-211 spectrometer. The lifetime τ of **1** was obtained as 37 μs via a single-exponential fit using the Origin software.
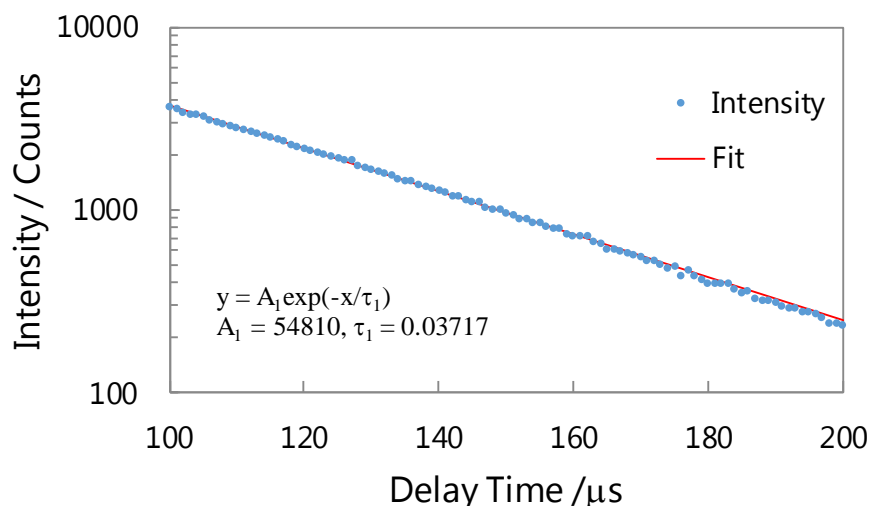

Figure S13. PL decay of **1** in cyclohexane at room temperature. The red line denotes the fit to the curve. The PL intensity at 570 nm was recorded (Excited at 320 nm).

PL lifetimes in the solid-state

Photoluminescence decay curves of **1G** and **1Y** were measured with a Hamamatsu photonics C11367-21 fluorescence lifetime spectrometer, with a Hamamatsu photonics C11567-02 Xe flash lamp unit for the phosphorescence measurements. The lifetime τ was obtained from a bi-exponential fit as implemented in the spectrometer's software. The PL intensities of **1G** and **1Y** were recorded at 520 nm and 570 nm, respectively (excitation was at 365 nm and 370 nm, respectively).

Table S3. PL Lifetimes of 1G and 1Y

sample	$<\tau>$ (μs)	τ_1 (μs)	τ_2 (μs)	A_1	A_2	χ^2
1G	101	39	109	161	442	1.10
1Y	51	32	78	137	38	1.09

The steady state PL spectrum of **1SC** at 77 K exhibited structured emission with λ_{em} = 522 and 561 nm, possibly due to the suppression of molecular vibration at low temperature (Figure S14). Time-gated phosphorescence spectrum with 10 ms delay after excitation was almost completely overlapped to the steady-state spectrum without shifts.
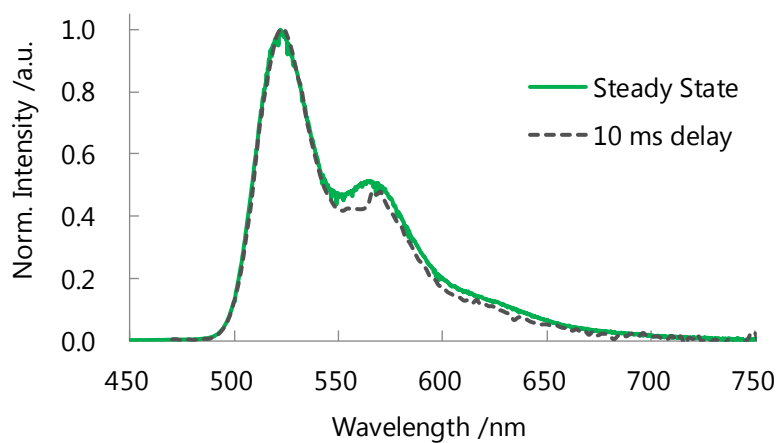

Figure S14. Steady state and delayed PL spectra of **1** single crystal at 77 K (λ_{ex} = 360 nm).

PL spectra of 3 in the solid-state

Photoluminescence spectra of **3** (crystalline and ground solid) were measured with a HORIBA Fluorolog3-211 spectrometer ($\lambda_{ex} = 400$ nm). The spectra did not change after grinding, confirming that **3** is not mechano-responsive (Figure S15). Note that the emission maximum of **3** were in between that of **1G** and **1Y**. In the single crystal, **3** took a planar conformation, which should be better regarded as a flattened skew conformer since the sulfur atom is *s-cis* to the proximal carbonyl oxygen atom (Figure S7). We assume that this planarization is responsible for the red-shifted spectra of **3** compared to that of **1G**.
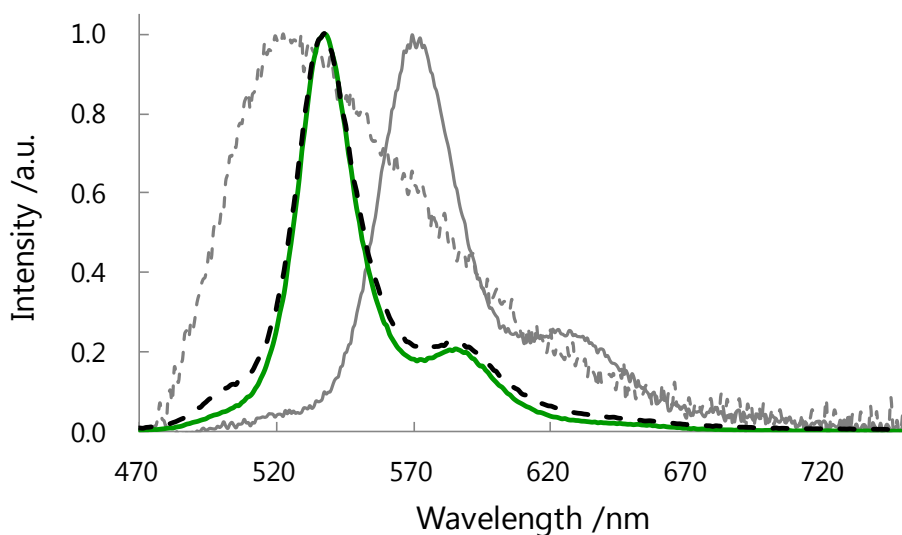

Figure S15. PL spectra of **3** crystal (green), its ground powder (black broken line), **1G** (grey broken line), and **1Y** (grey solid line).

6. Theoretical Calculations

All calculations were carried out using Gaussian 09 or 16 program packages.[6] Skew and TP conformers of thenils are denoted with subscripts "$_{SK}$" and "$_{TP}$", respectively.

All the geometry optimizations and frequency calculations were performed using the density functional theory (DFT) method for the S_0 and T_1 states, and the time-dependent (TD) DFT method for the S_1 state, at the B3LYP-D3/6-311G(d) level of theory unless otherwise noted.[7] Initial structures for the optimization in the S_0 state: for 1_{SK} and 2_{TP}, the experimental crystal structures; for 1_{TP}, the crystal structure of **1** with dihedral angles of O1–C5–C5a–O1a, S1–C4–C5–O1 and S1a–C4a–C5a–O1a modified to 180°; for 2_{SK}, the crystal structure of **1** with H in place of the triisopropylsilyl groups. The optimizations in the S_1 and T_1 states were started from the corresponding optimized structures in S_0. None of the optimized structures had imaginary frequencies.
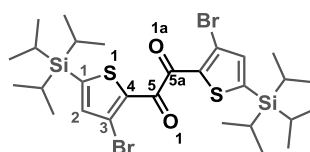
Suitable calculation methods for describing chalcogen bonding are still under discussion, and beyond the scope of this study. According to a review in 2018,[8] dispersion correction is crucial at least for *intermolecular* chalcogen bonding, and the B3LYP-D3 functional is recommended. In 2017, Cockroft et al. reported a calculation of a series of *intramolecular* chalcogen bonding. They pointed out that the experimental data were better reproduced without dispersion correction than with the correction.[9] We briefly surveyed the energy difference between 2_{SK} and 2_{TP} ($\Delta E_{SK–TP}$) as computed using several methods (Table S4). As a result, $\Delta E_{SK–TP}$ is found to be negative (2_{SK} is more stable) when calculated using dispersion-corrected DFT methods (entries 3–6). As discussed in the main text, UV-vis absorption spectrum of **1** suggested that the skew conformer is the dominant species in solution. Therefore, we have employed B3LYP-D3 as the calculation method in this work.

Table S4. Energy Difference between 2_{SK} and 2_{TP}

entry	method	$\Delta E_{SK–TP}$/kcal·mol^{-1}
1	B3LYP/6-311Gd	2.29
2	B3LYP/6-311Gd with PCM (cyclohexane)	1.79
3	B3LYP-D3/6-311Gd	−0.43
4	B3LYP-D3/6-311Gd with PCM (cyclohexane)	−0.99
5	ωB97X-D/6-311Gd	−1.44
6	M06-2X/6-311Gd	−0.29
7	MP2/cc-pVDZ	0.16

In the ground state, the optimized structure of $\mathbf{1_{TP}}$ has an S1–O1a distance of 2.71 Å and an C1–S1–O1a angle of 168.8°, which are in excellent agreement with those of $\mathbf{2_{TP}}$ (2.70 Å and 167.5°, respectively) and those of **2** single crystal (2.71 Å and 167.4°, respectively, Figure 5). The conformer $\mathbf{1_{SK}}$ is slightly more stable than $\mathbf{1_{TP}}$ by 0.79 kcal/mol.
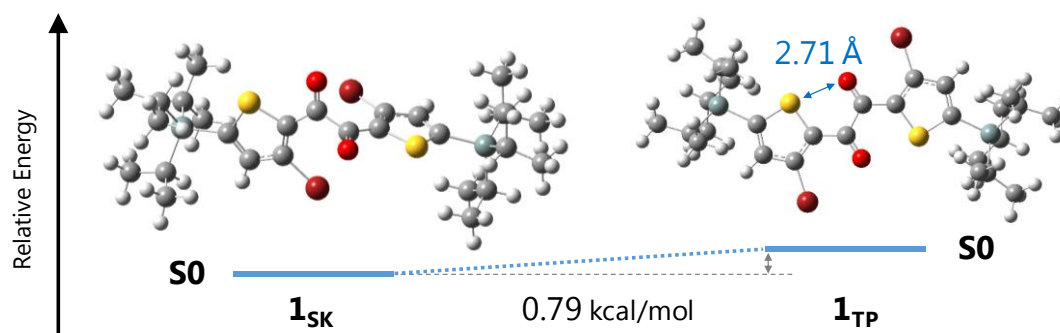

Figure S16. Optimized structures and relative energies of $\mathbf{1_{SK}}$ (left) and $\mathbf{1_{TP}}$ (right) in S_0.

Calculation for thenil **2** suggests that TP is a more stable conformer than the skew conformer in the excited states, and therefore the former would be the emissive species in solution (Figure S17). In the ground state, $\mathbf{2_{SK}}$ is slightly more stable than $\mathbf{2_{TP}}$ by 0.43 kcal/mol. Comparing the T_1 minima, in contrast, $\mathbf{2_{TP}}$ is much more stable than $\mathbf{2_{SK}}$ by 6.82 kcal/mol (Figure S17, bottom). Here, the structure of $\mathbf{2_{SK}}$ is relaxed with respect to the dihedral angle of the two carbonyls, from 94.1° in S_0 to 158.8° in T_1, although the thiophene rings are still twisted. For the S_1 state, the geometry optimization of $\mathbf{2_{SK}}$ did not converge. We compared the energies of Franck–Condon S_1 states through the TD-DFT single-point calculation for 20 excited states from the corresponding S_0-optimized structures. The calculation revealed that $\mathbf{2_{TP}}$ is more stable than $\mathbf{2_{SK}}$ by 16.4 kcal/mol at the Franck–Condon state (Figure S17, top).
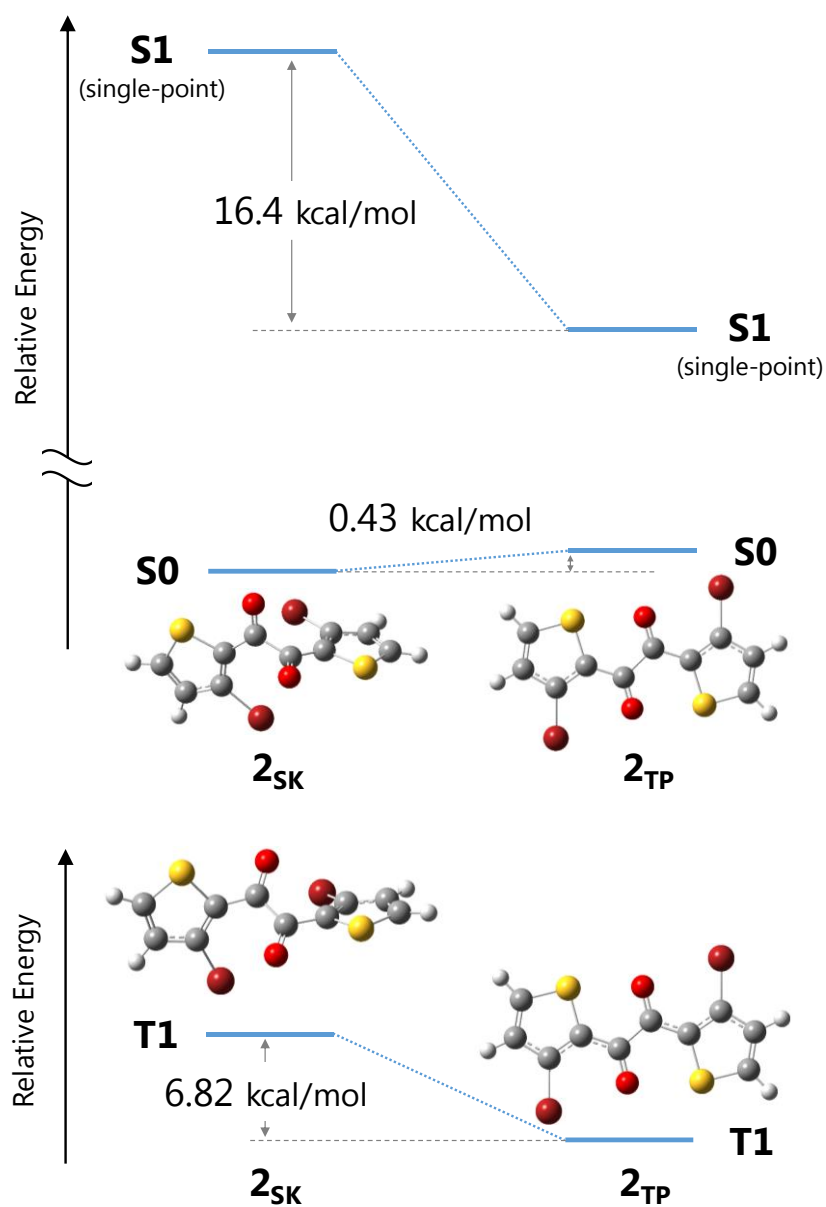
Figure S17. Optimized structures and relative energies of **2**$_{SK}$ (left) and **2**$_{TP}$ (right).
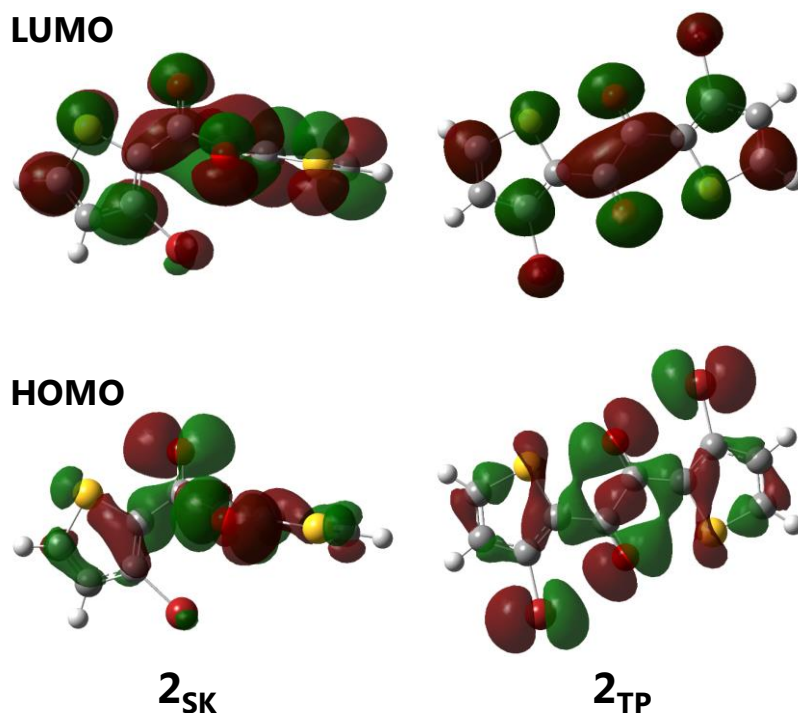
LUMO

HOMO

2_{SK} 2_{TP}

Figure S18. Kohn–Sham HOMOs and LUMOs of 2_{SK} (left) and 2_{TP} (right) in S_0.

Natural bonding orbital analysis of 2

The optimized structure of 2_{TP} at the B3LYP-D3/aug-cc-pVTZ level was subjected to natural bonding orbital (NBO) analysis[10] using a single-point energy calculation at the same level of theory. On the basis of second-order perturbation theory, donor–acceptor charge-transfer interactions were seen from both lone pairs orbitals (lp(1) and lp(2)) on the carbonyl oxygens to the S–C σ* orbitals, with the interaction energies of 0.90 and 2.97 kcal/mol, respectively. Since **2** has two chalcogen bonds, the total interaction energy is 7.74 kcal/mol.
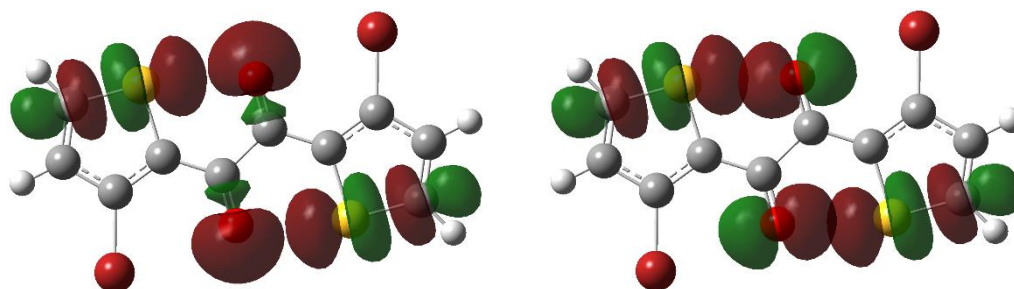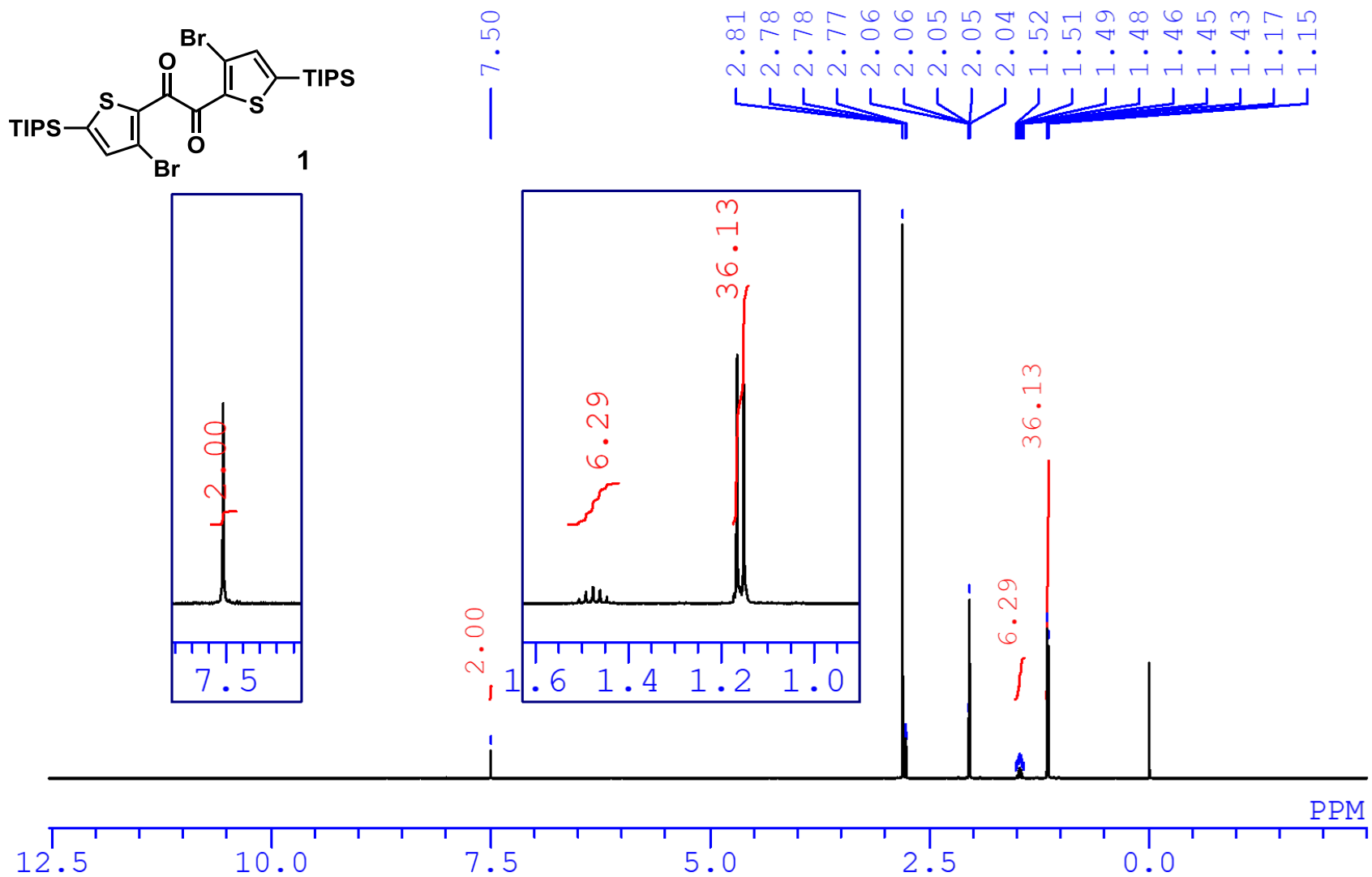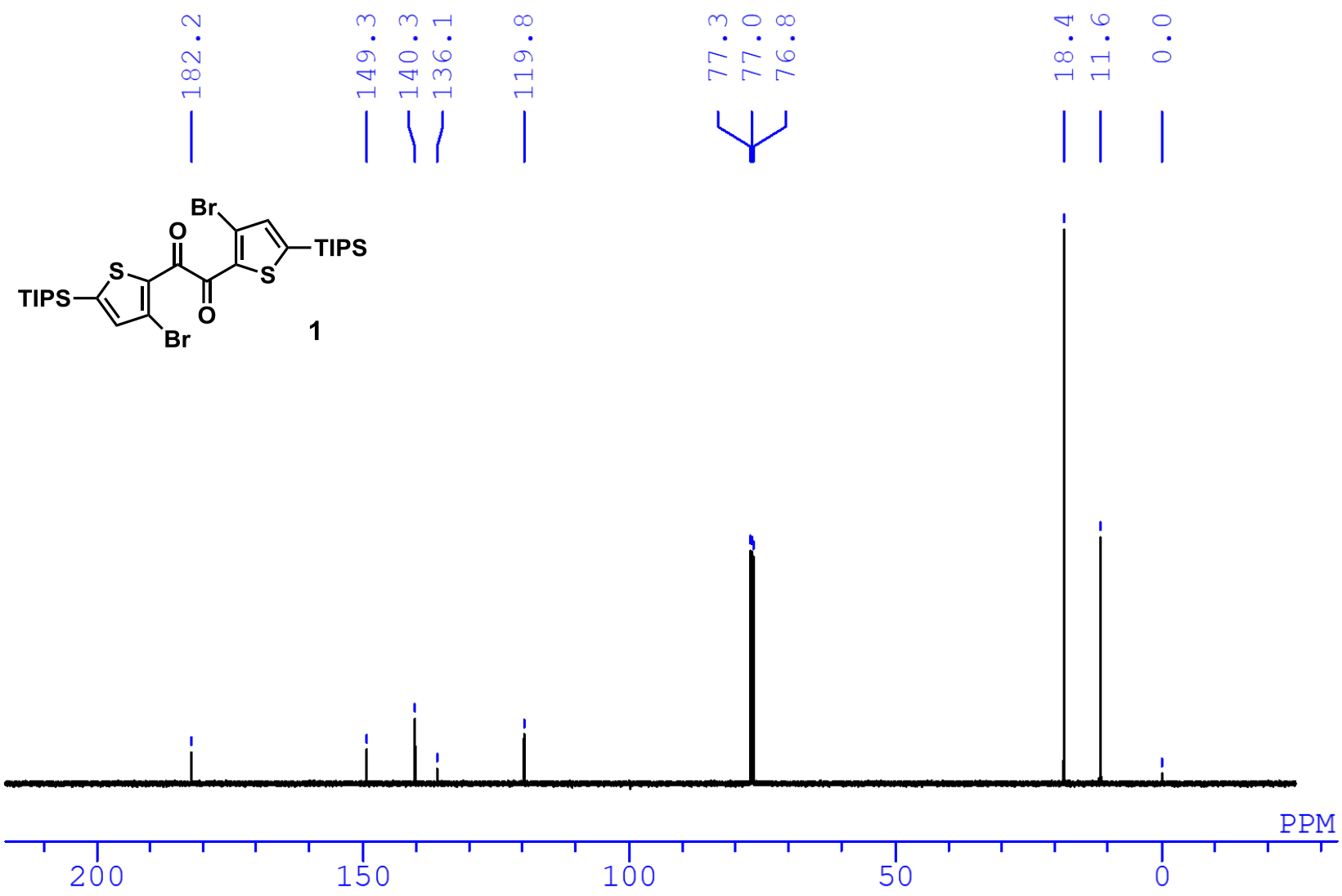

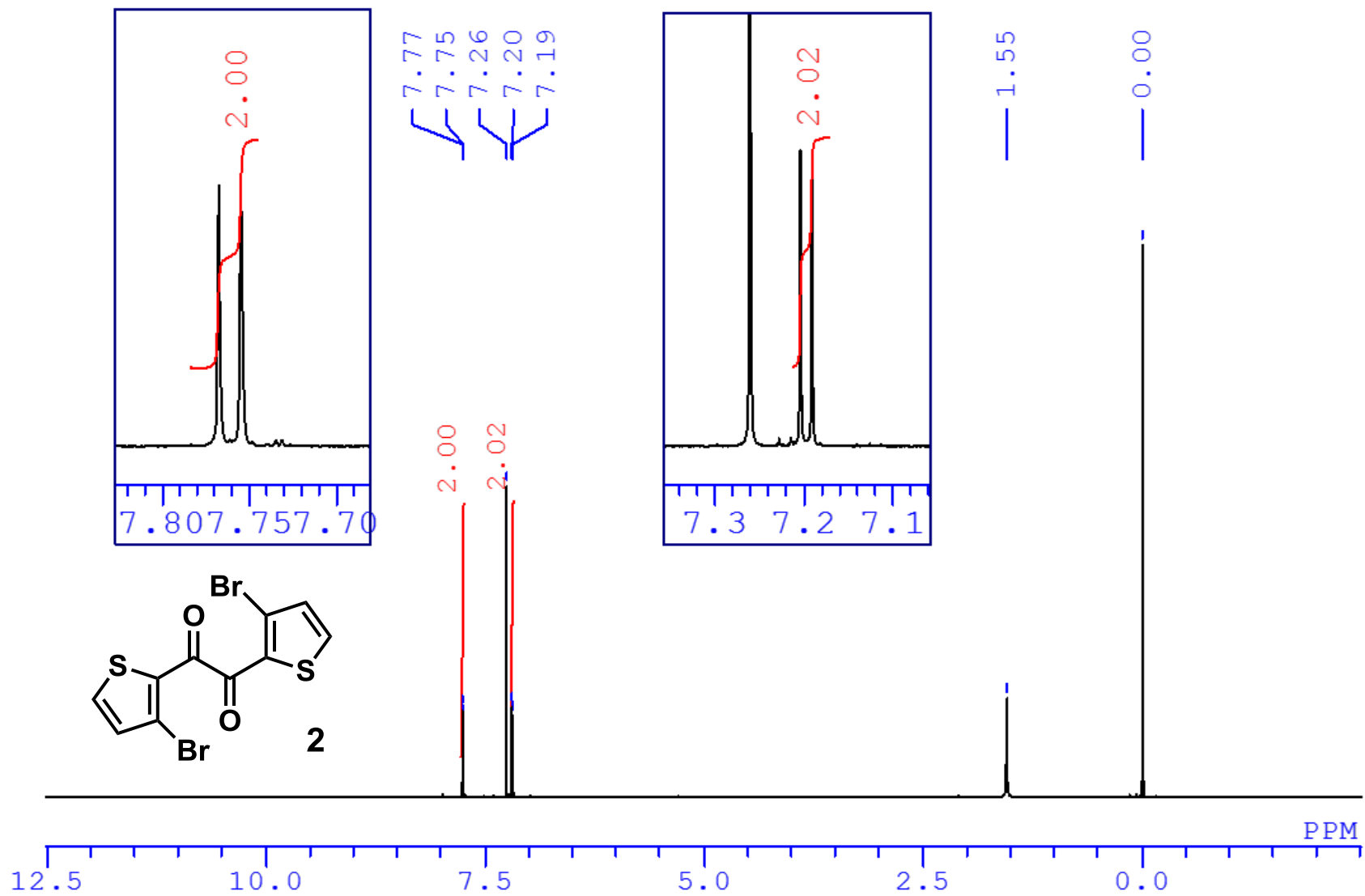**Figure S19.** Visual representation of the selected NBOs. Left, lp(1)→σ*; Right, lp(2)→σ*. Isovalue = 0.05.

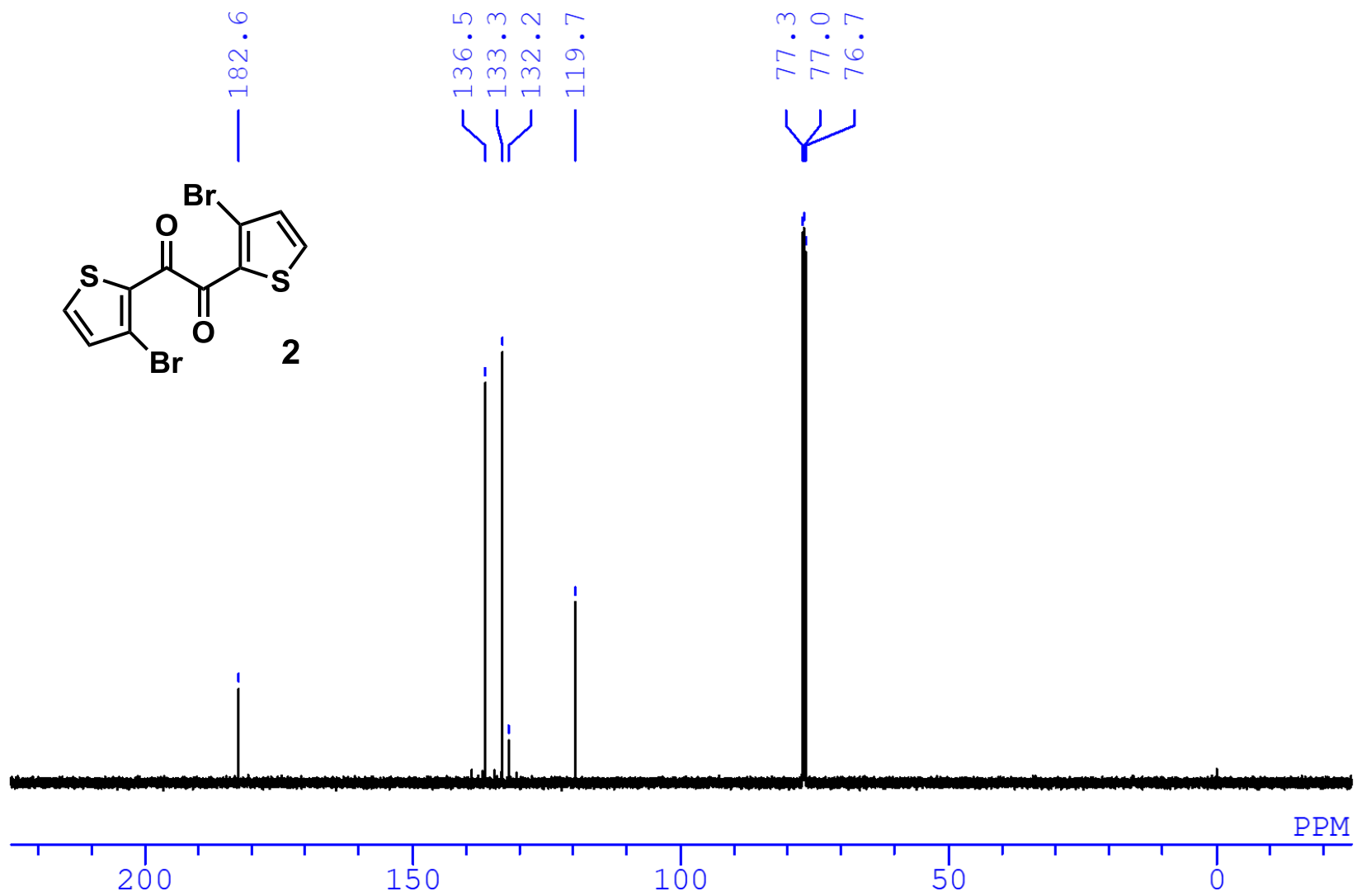**Calculation of the potential energy curves of 2 (Figure 4)**

As an initial attempt, we scanned the reaction coordinate along the dihedral angle of the two carbonyls. However, this did not allow us to obtain the other isomer. Whereas, a 2D-scan along the two dihedrals around the thiophene–carbonyl bonds revealed the presence of a metastable intermediate conformer, **2$_{INT}$**. The geometry optimization and frequency calculation of **2$_{INT}$** found a stationary point without imaginary frequencies. From this optimized **2$_{INT}$** initial structure, we scanned the coordinate around one of two thiophene–carbonyl bonds. The step of the scan was set to 20°. At each point, a single-point calculation was performed to obtain the S$_1$ and T$_1$ energy levels. From the results we confirmed that TP is far more stable than the skew conformer in the excited states.
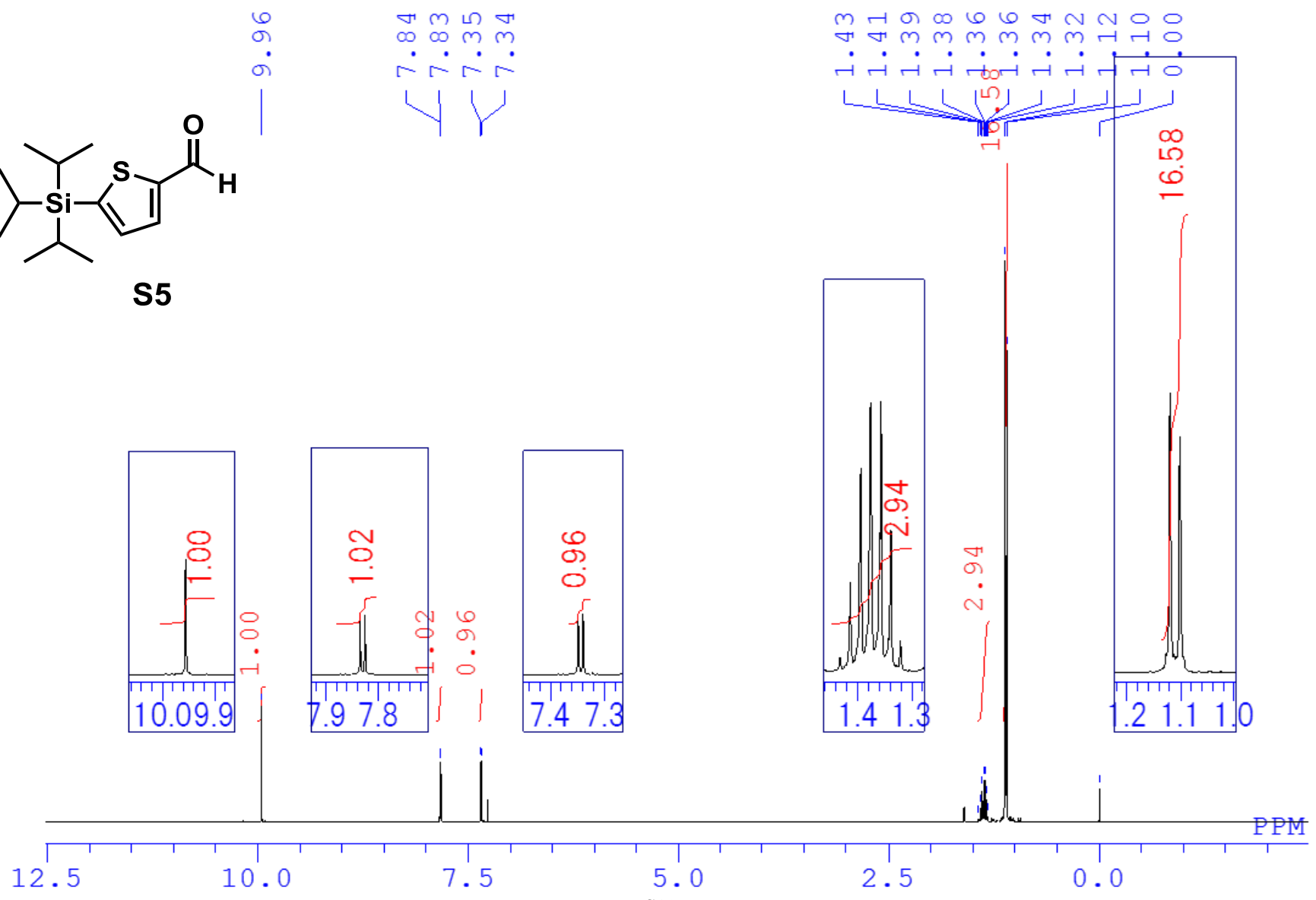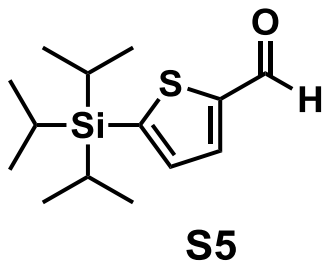
7. NMR Charts

182.2
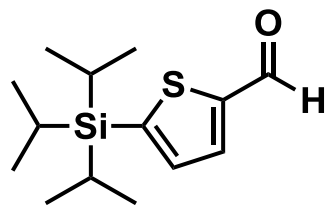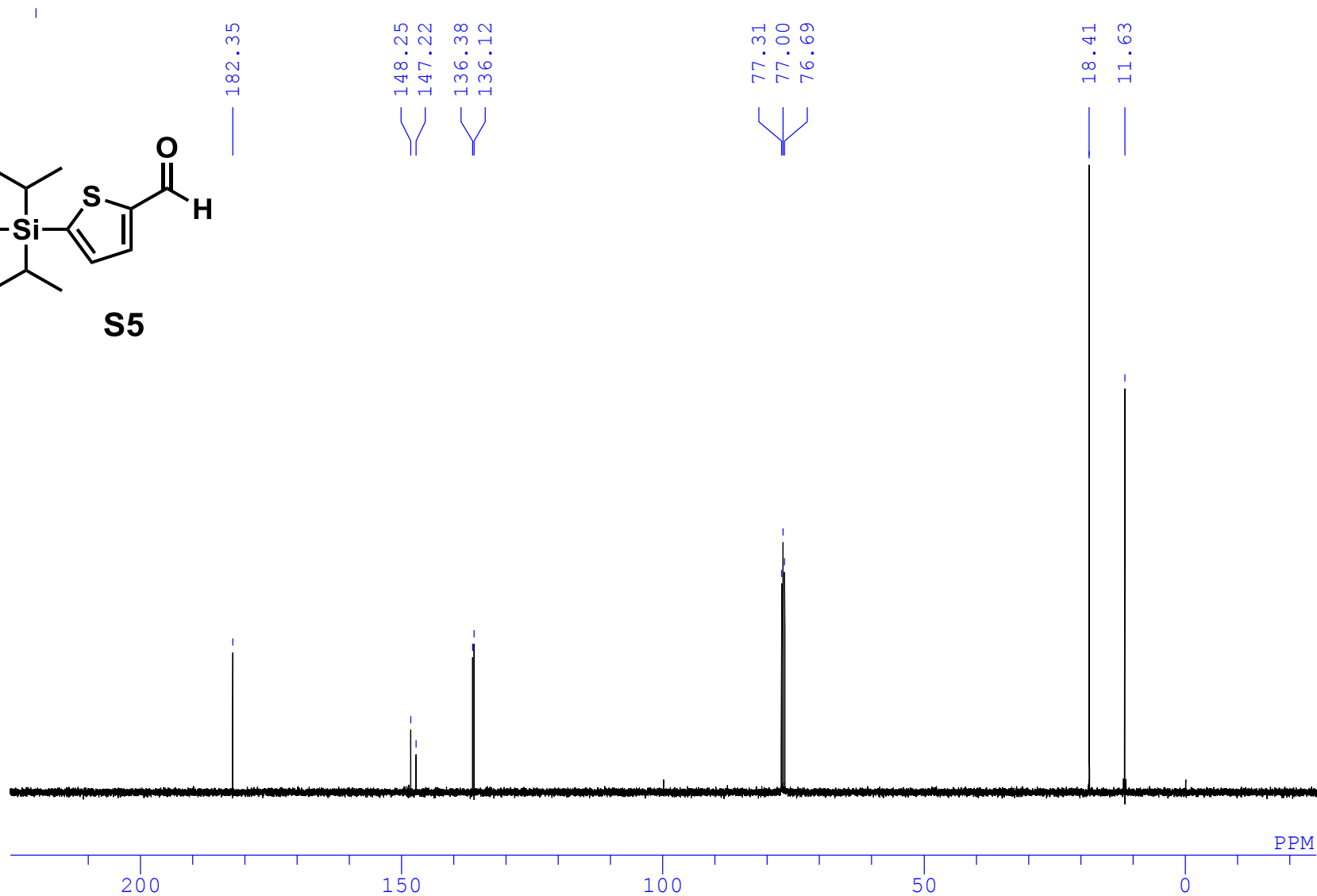149.3
140.3
136.1
119.8
77.3
77.0
76.8
18.4
11.6
0.0

1

200   150   100   50   0   PPM

S29

7.77
7.75
7.26
7.20
7.19

2.00

2.02

2.00

2.02

1.55

0.00

7.80 7.75 7.70

7.3 7.2 7.1

2

PPM

12.5   10.0   7.5   5.0   2.5   0.0

S31

S5

9.96

7.84 7.83 7.35 7.34

1.43 1.41 1.39 1.38 1.36 1.36 1.34 1.32 1.12 1.10 0.00

1.58

16.58

1.00

1.02

0.96

2.94

2.94

16.58

1.00

1.02

0.96

10.0 9.9

7.9 7.8

7.4 7.3

1.4 1.3

1.2 1.1 1.0

12.5   10.0   7.5   5.0   2.5   0.0   PPM

S32

182.35

148.25
147.22
136.38
136.12

77.31
77.00
76.69

18.41
11.63

S5

200   150   100   50   0   PPM

S33

S6

S34

S6

182.64

150.08
143.16
137.23
136.49

77.31
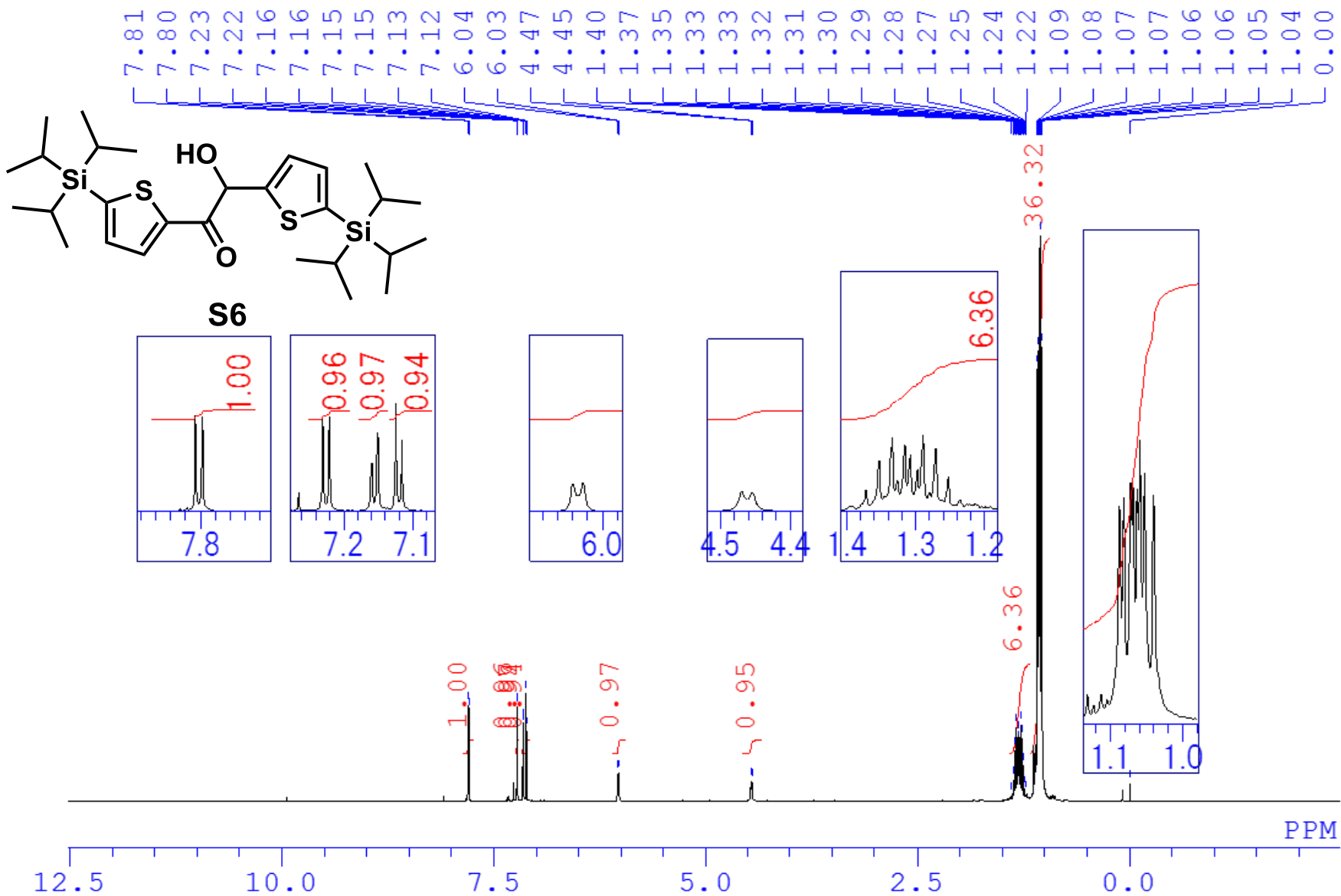77.00
76.69

18.45
11.68

3
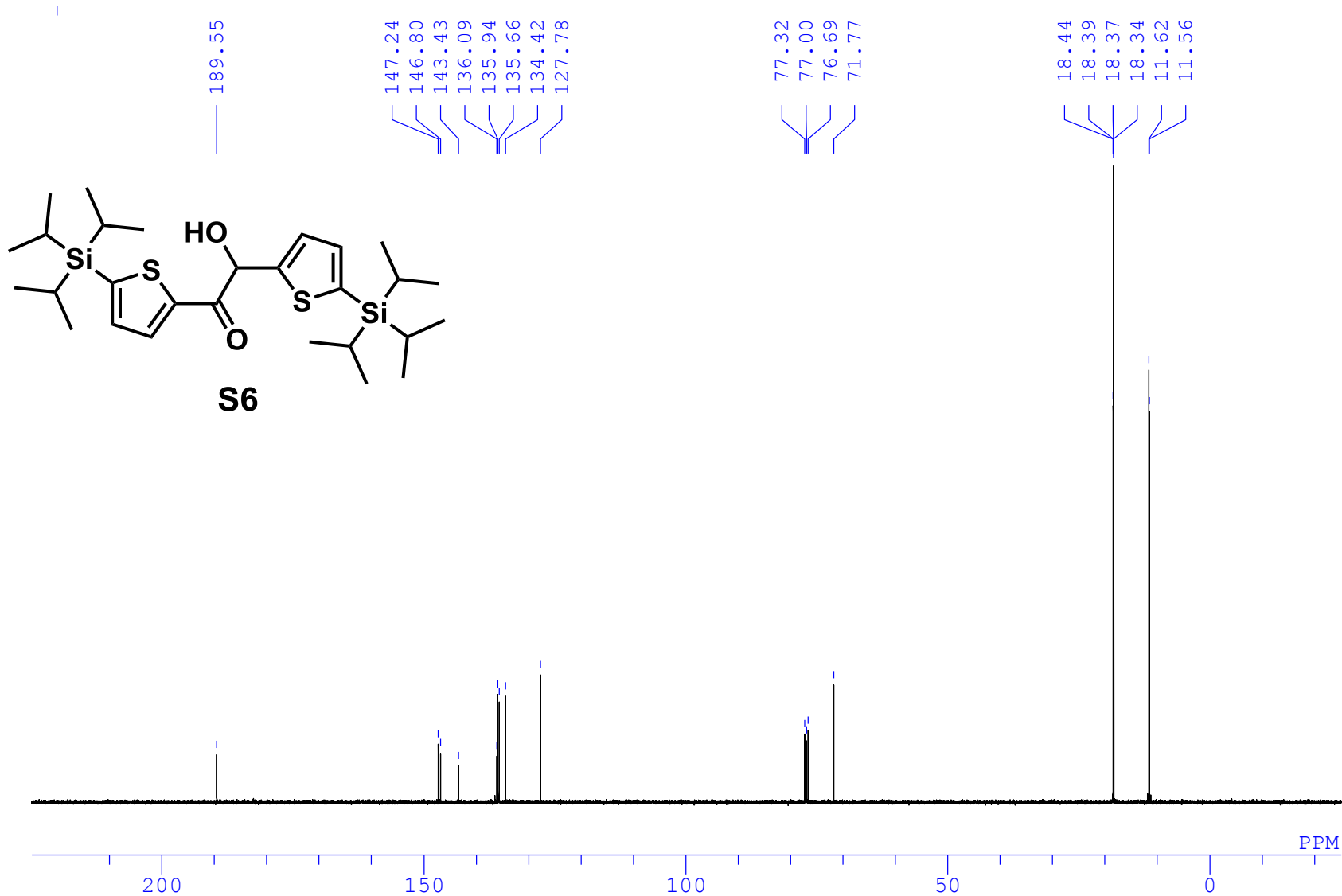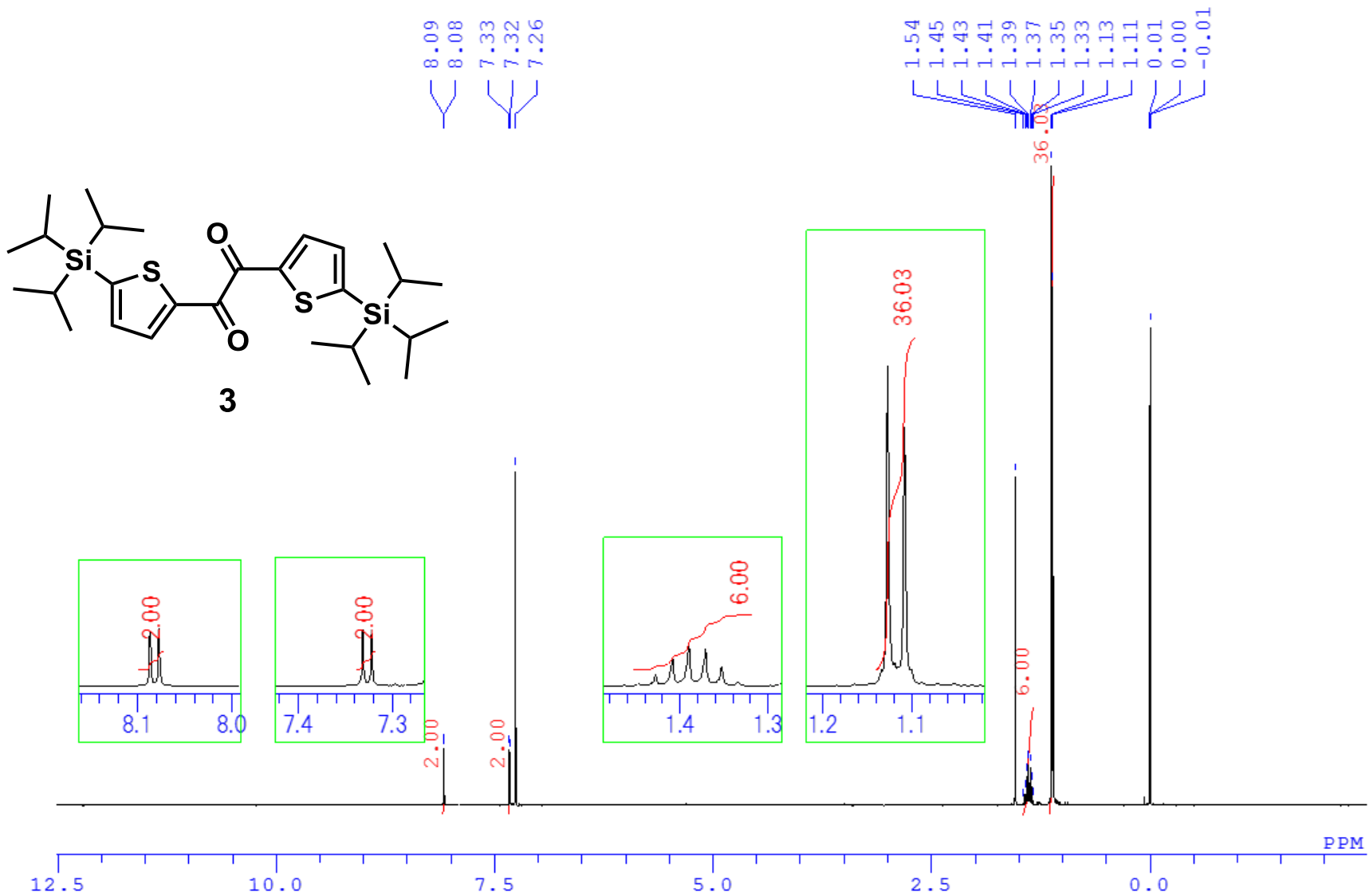
PPM

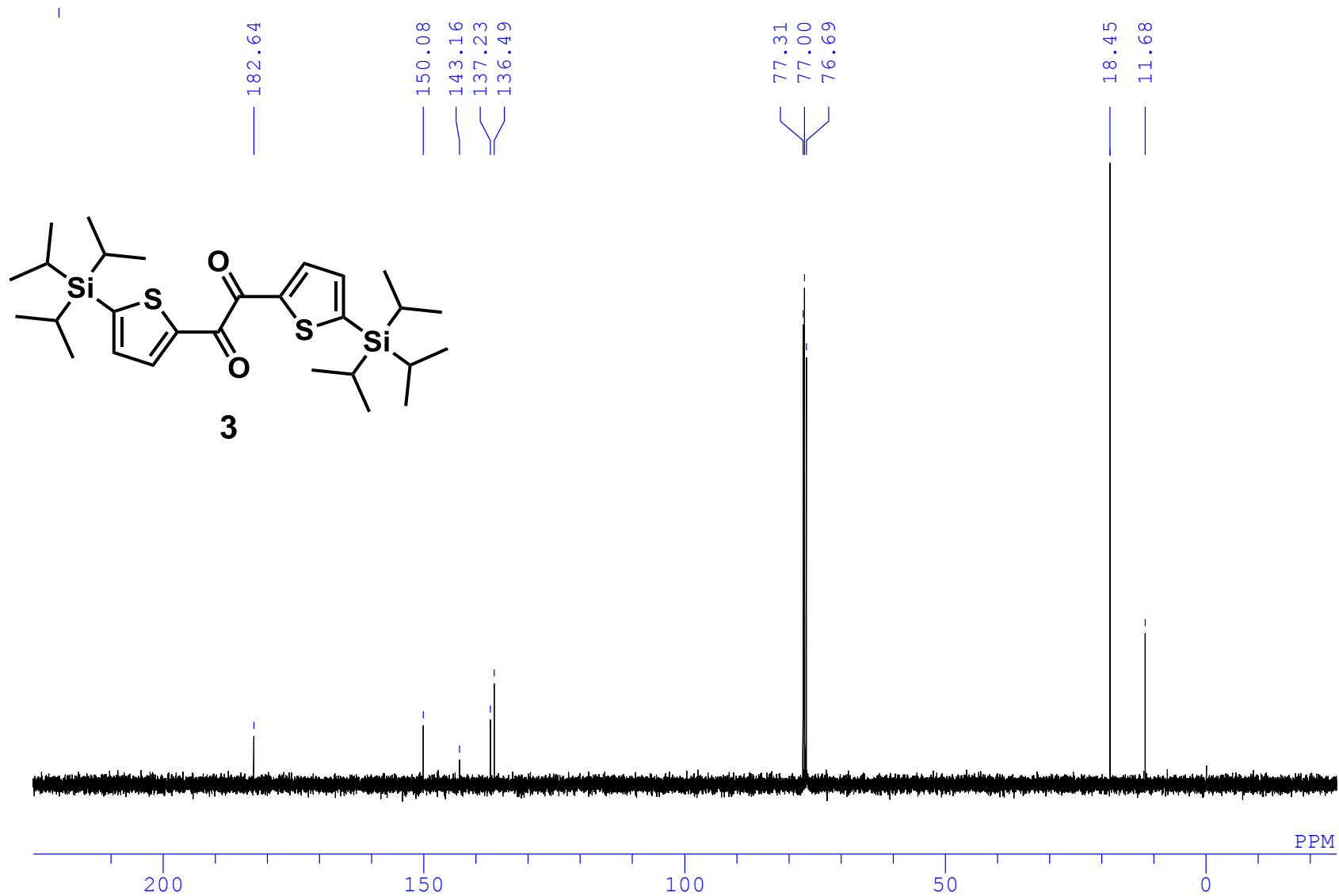200   150   100   50   0

S37

8. References

1. (a) K. Suzuki, A. Kobayashi, S. Kaneko, K. Takehira, T. Yoshihara, H. Ishida, Y. Shiina, S. Oishi and S. Tobita, *Phys. Chem. Chem. Phys.*, 2009, **11**, 9850–9860; (b) A. M. Brouwer, *Pure Appl. Chem.*, 2011, **83**, 2213-2228.

2. A. B. Pangborn, M. A. Giardello, R. H. Grubbs, R. K. Rosen and F. J. Timmers, *Organometallics*, 1996, **15**, 1518-1520.

3. Y. Tani and T. Ogawa, *Org. Lett.*, 2018, **20**, 7442-7446.

4. A. Blencowe, A. M. Celli, D. Donati, W. C. Hayes, C. Martin, P. J. Murphy, F. Ponticelli and J. K. Melville-Richards, *Tetrahedron*, 2009, **65**, 3858-3862.

5. P.-J. Zhou, C.-K. Li, S.-F. Zhou, A. Shoberu and J.-P. Zou, *Org. Biomol. Chem.*, 2017, **15**, 2629-2637.

6. (a) M. J. Frisch, G. W. Trucks, H. B. Schlegel, G. E. Scuseria, M. A. Robb, J. R. Cheeseman, G. Scalmani, V. Barone, B. Mennucci, G. A. Petersson, H. Nakatsuji, M. Caricato, X. Li, H. P. Hratchian, A. F. Izmaylov, J. Bloino, G. Zheng, J. L. Sonnenberg, M. Hada, M. Ehara, K. Toyota, R. Fukuda, J. Hasegawa, M. Ishida, T. Nakajima, Y. Honda, O. Kitao, H. Nakai, T. Vreven, J. A. Montgomery Jr., J. E. Peralta, F. Ogliaro, M. Bearpark, J. J. Heyd, E. Brothers, K. N. Kudin, V. N. Staroverov, R. Kobayashi, J. Normand, K. Raghavachari, A. Rendell, J. C. Burant, S. S. Iyengar, J. Tomasi, M. Cossi, N. Rega, J. M. Millam, M. Klene, J. E. Knox, J. B. Cross, V. Bakken, C. Adamo, J. Jaramillo, R. Gomperts, R. E. Stratmann, O. Yazyev, A. J. Austin, R. Cammi, C. Pomelli, J. W. Ochterski, R. L. Martin, K. Morokuma, V. G. Zakrzewski, G. A. Voth, P. Salvador, J. J. Dannenberg, S. Dapprich, A. D. Daniels, Ö. Farkas, J. B. Foresman, J. V. Ortiz, J. Cioslowski and D. J. Fox, *Gaussian 09 Rev. C.01*, Wallingford, CT, 2009; (b) M. J. Frisch, G. W. Trucks, H. B. Schlegel, G. E. Scuseria, M. A. Robb, J. R. Cheeseman, G. Scalmani, V. Barone, G. A. Petersson, H. Nakatsuji, X. Li, M. Caricato, A. V. Marenich, J. Bloino, B. G. Janesko, R. Gomperts, B. Mennucci, H. P. Hratchian, J. V. Ortiz, A. F. Izmaylov, J. L. Sonnenberg, Williams, F. Ding, F. Lipparini, F. Egidi, J. Goings, B. Peng, A. Petrone, T. Henderson, D. Ranasinghe, V. G. Zakrzewski, J. Gao, N. Rega, G. Zheng, W. Liang, M. Hada, M. Ehara, K. Toyota,

R. Fukuda, J. Hasegawa, M. Ishida, T. Nakajima, Y. Honda, O. Kitao, H. Nakai, T. Vreven, K. Throssell, J. A. Montgomery Jr., J. E. Peralta, F. Ogliaro, M. J. Bearpark, J. J. Heyd, E. N. Brothers, K. N. Kudin, V. N. Staroverov, T. A. Keith, R. Kobayashi, J. Normand, K. Raghavachari, A. P. Rendell, J. C. Burant, S. S. Iyengar, J. Tomasi, M. Cossi, J. M. Millam, M. Klene, C. Adamo, R. Cammi, J. W. Ochterski, R. L. Martin, K. Morokuma, O. Farkas, J. B. Foresman and D. J. Fox, *Gaussian 16 Rev. B.01*, Wallingford, CT, 2016.

7.   S. Grimme, J. Antony, S. Ehrlich and H. Krieg, *J. Chem. Phys.*, 2010, **132**, 154104.

8.   R. Gleiter, G. Haberhauer, D. B. Werz, F. Rominger and C. Bleiholder, *Chem. Rev.*, 2018, **118**, 2010-2041.

9.   D. J. Pascoe, K. B. Ling and S. L. Cockroft, *J. Am. Chem. Soc.*, 2017, **139**, 15160-15167.

10.   E. D. Glendening, J. K. Badenhoop, A. E. Reed, J. E. Carpenter, J. A. Bohmann, C. M. Morales, C. R. Landis and F. Weinhold, *NBO 6.0*, Theoretical Chemistry Institute, University of Wisconsin, Madison, WI, 2013.